

2017 Fall

“Phase Transformation *in* Materials”

10.30.2017

Eun Soo Park

Office: 33-313

Telephone: 880-7221

Email: espark@snu.ac.kr

Office hours: by an appointment

Contents for previous class

Chapter 3 Crystal Interfaces and Microstructure

1) Interfacial Free Energy (γ : J/m²)

→ The Gibbs free energy of a system containing an interface of area A

→ $G_{\text{bulk}} + G_{\text{interface}}$ vapor
solid $G = G_0 + \gamma A$ → $F = \gamma + A d\gamma/dA$ (liq. : $d\gamma/dA = 0$)

* Origin of the **surface free energy (E_{sv})**? → **Broken Bonds**

2) Solid/Vapor Interfaces

$high T_m \rightarrow high L_s \rightarrow high \gamma_{sv}$

* γ interfacial energy = free energy (J/m²) γ - θ plot

→ $\gamma = G = H - TS$

$= E + PV - TS$ (: PV is ignored)

→ $\gamma = E_{sv} - TS_{sv}$ (S_{sv} thermal entropy, configurational entropy)

→ $\partial\gamma/\partial T = -S$: surface energy decreases with increasing T

$\sum_{i=1}^n A_i \gamma_j = \text{Minimum}$

Equilibrium shape: Wulff surface

$E_{sv} = 3 \epsilon/2 = 0.25 L_s / N_a$ ⇒ $\gamma_{sv} = 0.15 L_s / N_a$ J / surface atom 2

(∵ surface free Es averaged over many surface plane, S effect at high T)

Surface energy for high or irrational {hkl} index

Closer surface packing \rightarrow smaller number of broken bond \rightarrow lower surface energy
 # of broken bonds will increase through the series {111} {200} {220} \rightarrow γ_{SV} will increase along the same series (if different entropy term is ignored)

A crystal plane at an angle θ to the close-packed plane will contain broken bonds in excess of the close-packed plane due to the atoms at the steps.

Surface with high {hkl} index

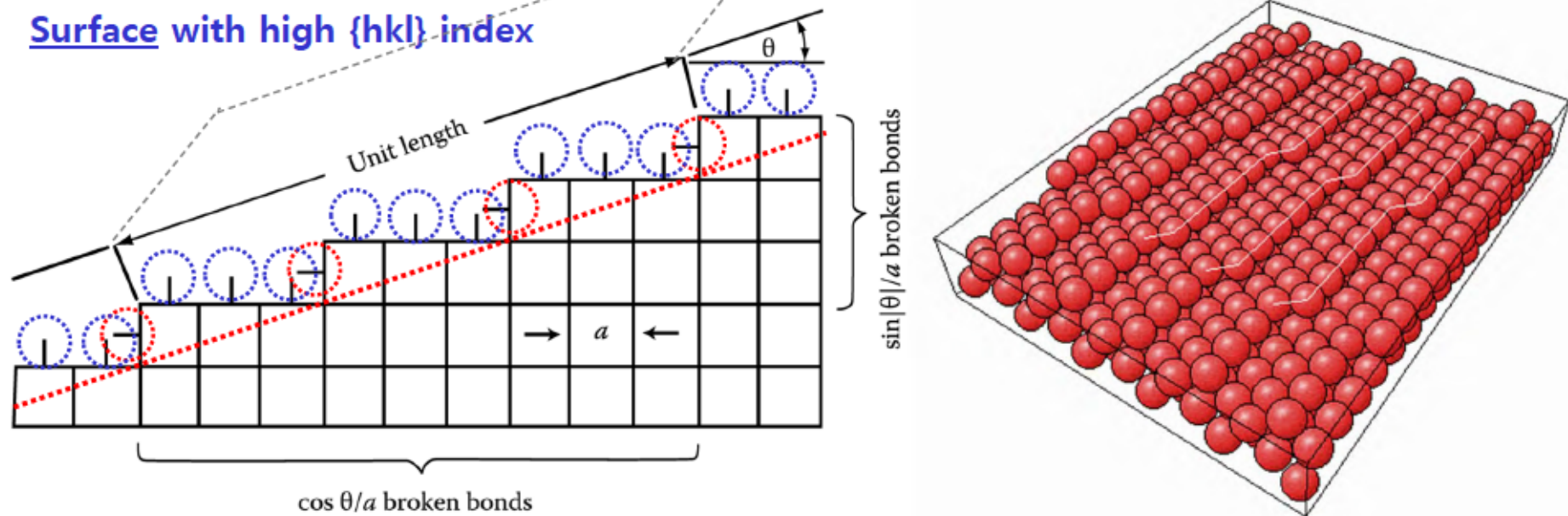


Fig. 2.2 The 'broken-bond' model for surface energy.

**$(\cos\theta/a)(1/a)$: broken bonds
 from the atoms on the steps**

**$(\sin|\theta|/a)(1/a)$: additional broken bonds
 from the atoms on the steps**

Surface energy for high or irrational {hkl} index

$(\cos\theta/a)(1/a)$: broken bonds from the atoms on the steps

$(\sin|\theta|/a)(1/a)$: additional broken bonds from the atoms on the steps

Attributing $\varepsilon/2$ energy to each broken bond,

$$E_{SV} = \frac{1}{1 \times a} \frac{\varepsilon}{2} \left(\frac{\cos\theta}{a} + \frac{\sin|\theta|}{a} \right)$$
$$= \frac{\varepsilon(\cos\theta + \sin(|\theta|))}{2a^2}$$

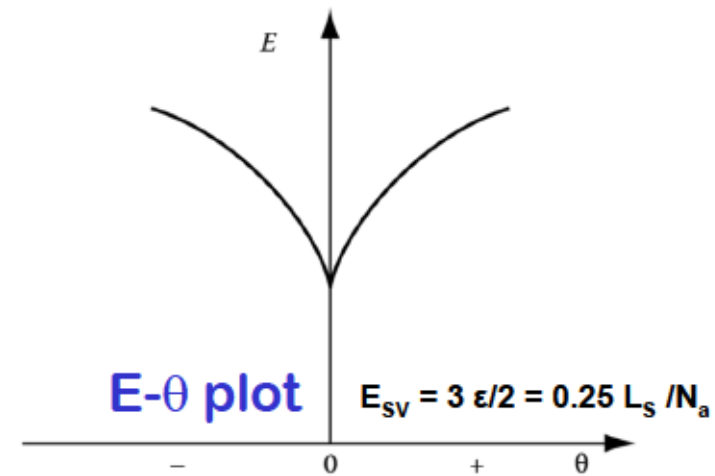


Fig. 3.4 Variation of surface energy as a function of θ

- The close-packed orientation ($\theta = 0$) lies at a cusped minimum in the E plot.
- Similar arguments can be applied to any crystal structure for rotations about any axis from any reasonably close-packed plane.
- All low-index planes should therefore be located at low-energy cusps.
- If γ is plotted versus θ similar cusps are found (γ - θ plot), but as a result of entropy effects they are less prominent than in the E - θ plot, and for the higher index planes they can even disappear.

Q: Free surface (solid/vapor interface)?

(a) E_{SV} vs γ ?

Extra energy per atom on surface

- The measured γ values for pure metals near the melting temperature

$$E_{SV} = 3 \epsilon/2 = 0.25 L_S / N_a \quad \Rightarrow \quad \gamma_{SV} = 0.15 L_S / N_a \quad \text{J / surface atom}$$

(\because surface free E averaged over many surface plane, S effect at high T)

(b) Equilibrium shape: Wulff surface

: Polyhedron with the largest facets having the lowest interfacial free energy

Equilibrium shape: Wulff surface

* A convenient method for plotting the variation of γ with surface orientation in 3 dimensions

* **Distance from center** : γ_{sv}

→ Construct the surface using γ_{sv} value as a distance between the surface and the origin when measured along the normal to the plane

Several plane A_1, A_2 etc. with energy γ_1, γ_2

Total surface energy : $A_1\gamma_1 + A_2\gamma_2, \dots$

= $\sum A_i \gamma_i \rightarrow$ minimum

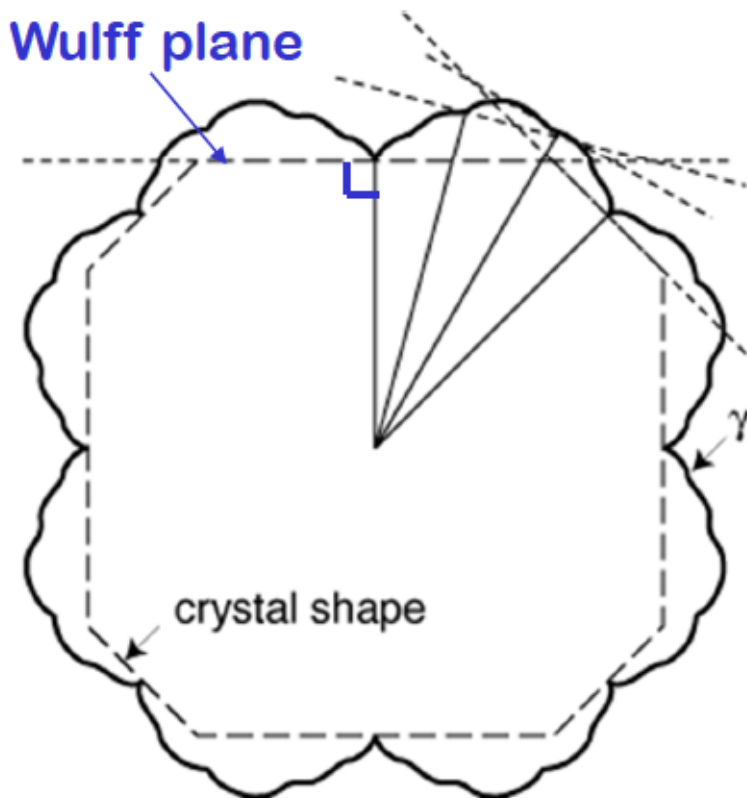
→ equilibrium morphology

: can predict the equilibrium shape of
an isolated single crystal

How is the equilibrium shape
determined?

$$\sum_{i=1}^n A_i \gamma_j = \text{Minimum}$$

Wulff plane



γ - θ plot

Due to entropy effects the plot are less prominent than in the E_{sv} - θ plot, and for the higher index planes they can even disappear

Process of Wulff shape intersection for two cubic Wulff shapes
: Polyhedron with the largest facets having the lowest interfacial free energy

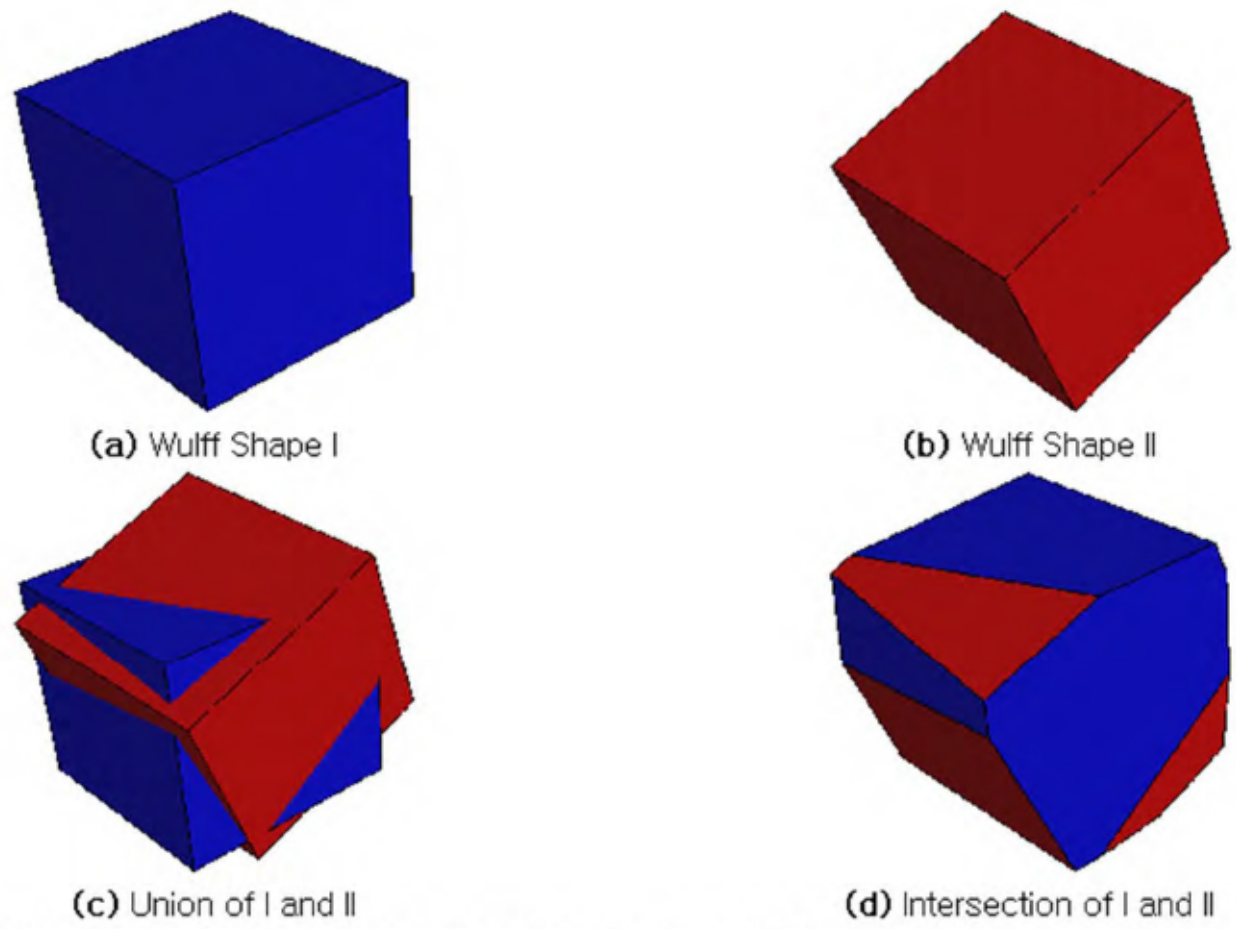
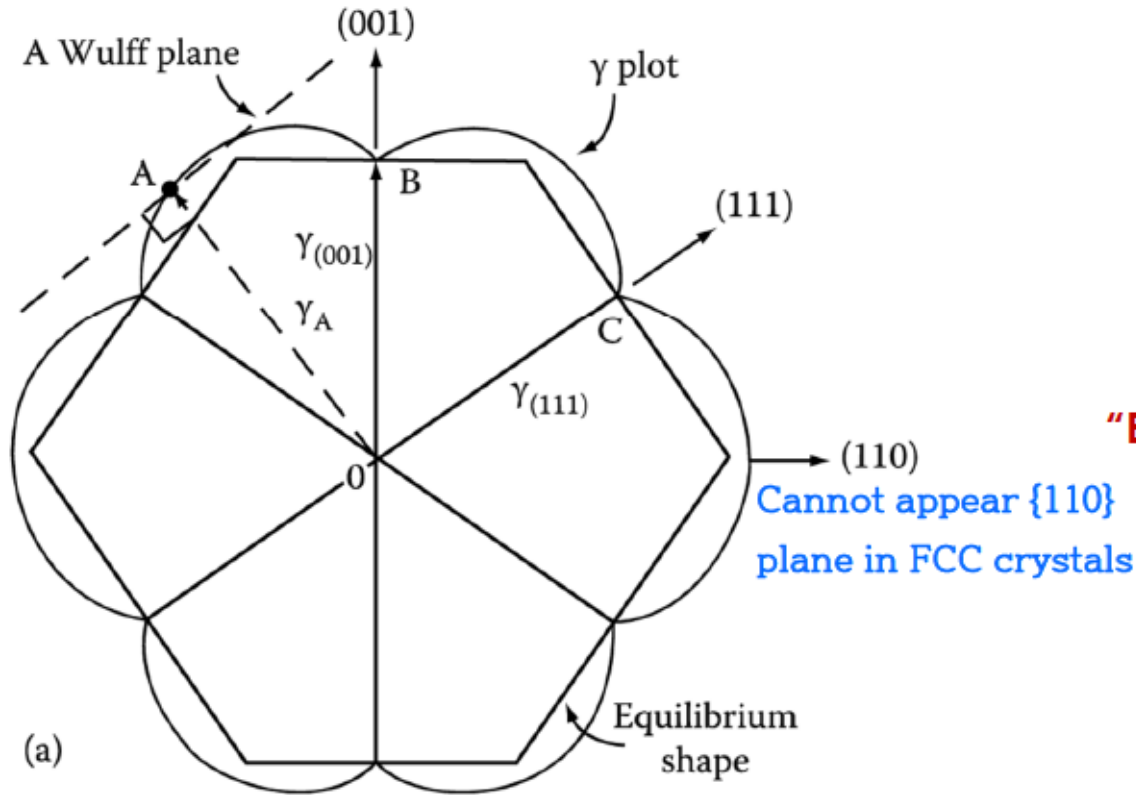


Figure 1: The process of Wulff shape intersection for two cubic Wulff shapes with displaced origins and rotated coordinate systems. Each individual shape has cubic symmetry $m\bar{3}m$ and $[100]$ facets.

Equilibrium shape: Wulff surface

Equilibrium shape can be determined experimentally by annealing small single crystals at high temperatures in an inert atmosphere, or by annealing small voids inside a crystal.

Of course **when γ is isotropic**, as for liquid droplets, both the γ -plots and equilibrium shapes are **spheres**.



“Equilibrium shape of FCC crystals”

- 1) Square faces $\{100\}$ and
- 2) Hexagonal faces $\{111\}$

The length OA represents the free energy of a surface plane whose normal lies in the direction OA .

A possible $(\bar{1}10)$ section through the γ -plot of an fcc crystal

Q: Grain boundary (α/α interfaces)

= Boundaries in Single-Phase Solids

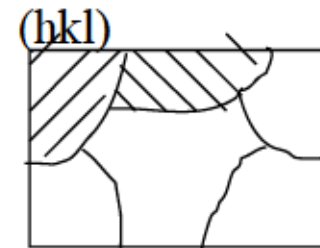
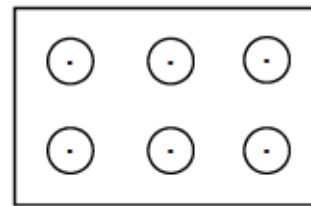
(a) Low-Angle and High-Angle Boundaries

(b) Special High-Angle Grain Boundaries

(c) Equilibrium in Polycrystalline Materials

3.3 Boundaries in Single-Phase Solids: definition

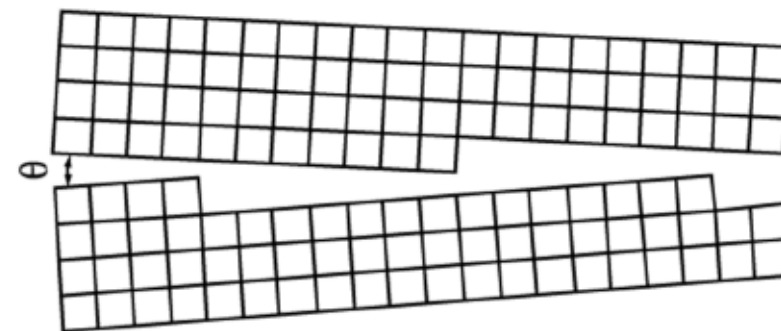
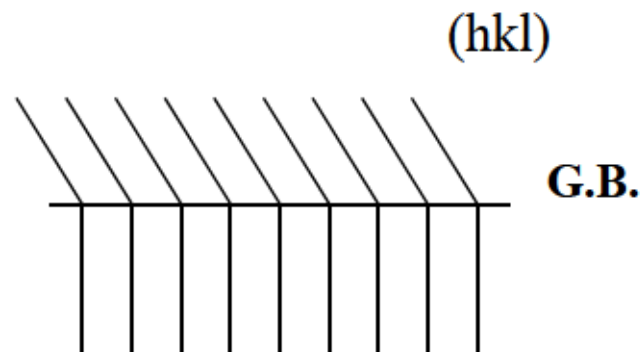
Grain boundary (α/α interfaces)



Single phase - Poly grain

> same composition, same crystal structure

> different orientation



1) misorientation of the two adjoining grains

두 개 인접한 결정립간 방위차이 cf. 두 조밀면 만남

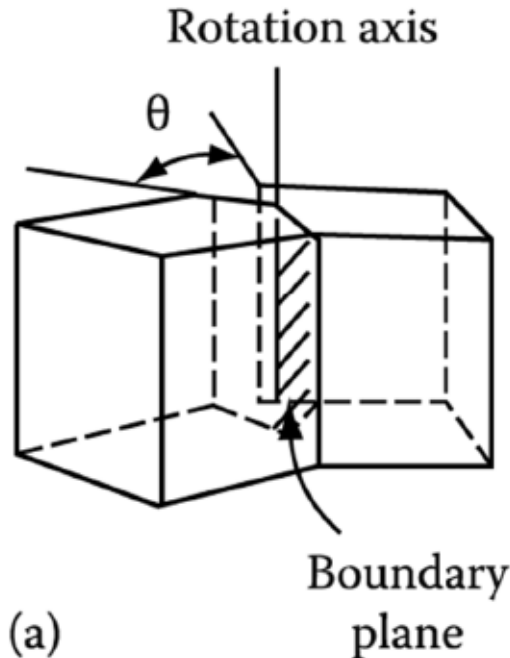
2) orientation of the boundary plane

인접 결정립과 입계면의 방위관계

3.3 Boundaries in Single-Phase Solids

: The lattices of any two grains can be made to coincide by rotating one of them through a suitable angle about a single axis.

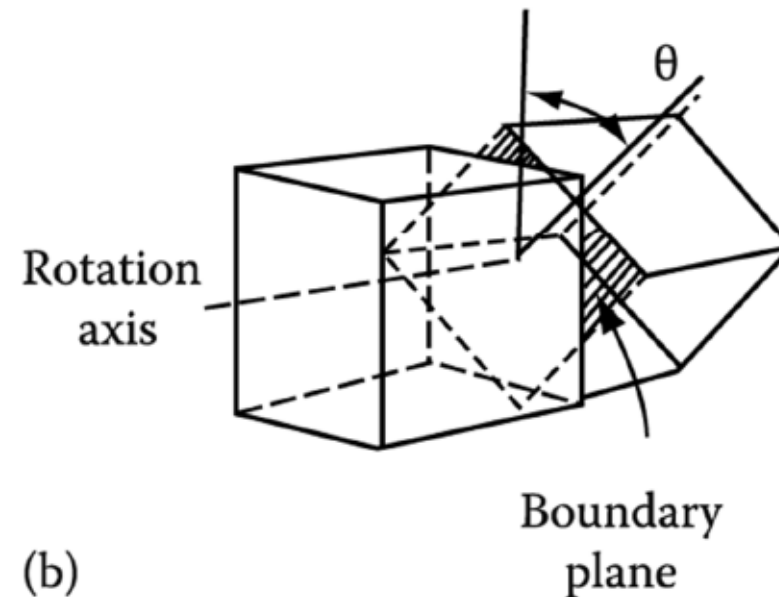
* Relatively simple boundary: relative orientation of the crystals and the boundary



tilt boundary

$\theta \rightarrow$ **misorientation**
 \rightarrow **tilt angle**

Axis of rotation: **parallel to the plane of the boundary**



twist boundary

$\theta \rightarrow$ **misorientation**
 \rightarrow **twist angle**

Perpendicular to the boundary

[**symmetric tilt or twist boundary**
non-symmetric tilt or twist boundary

3.3.1 Low-Angle and High-Angle Boundaries

Low-Angle Boundaries

Symmetrical low-angle tilt boundary

Symmetrical low-angle twist boundary

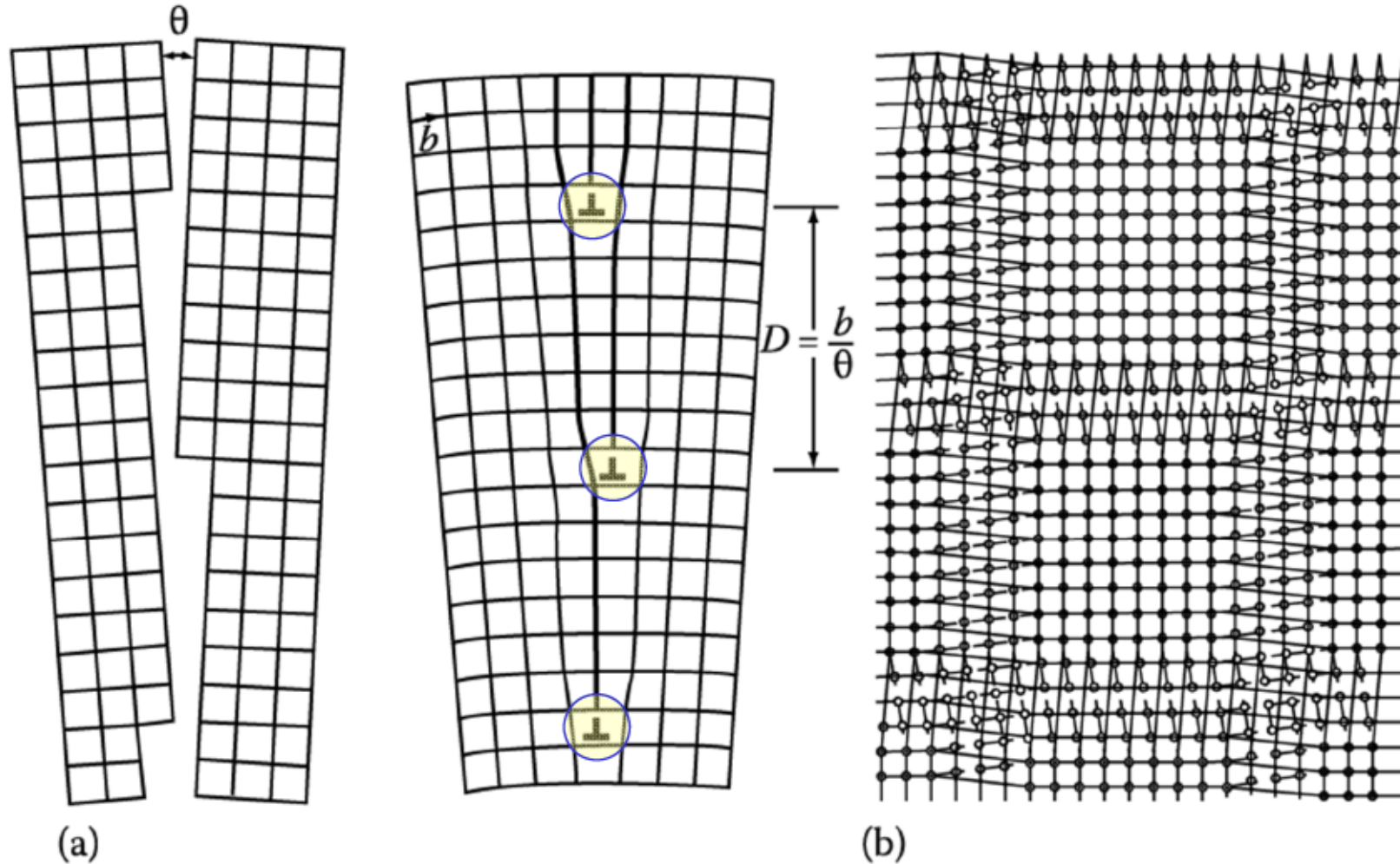


Fig. 3.7 (a) Low-angle tilt boundary, (b) low-angle twist boundary: ○ atoms in crystal below, ● atoms in crystal above boundary.

An array of parallel edge dislocation

Cross-grid of two sets of screw dislocations

tilt Boundaries

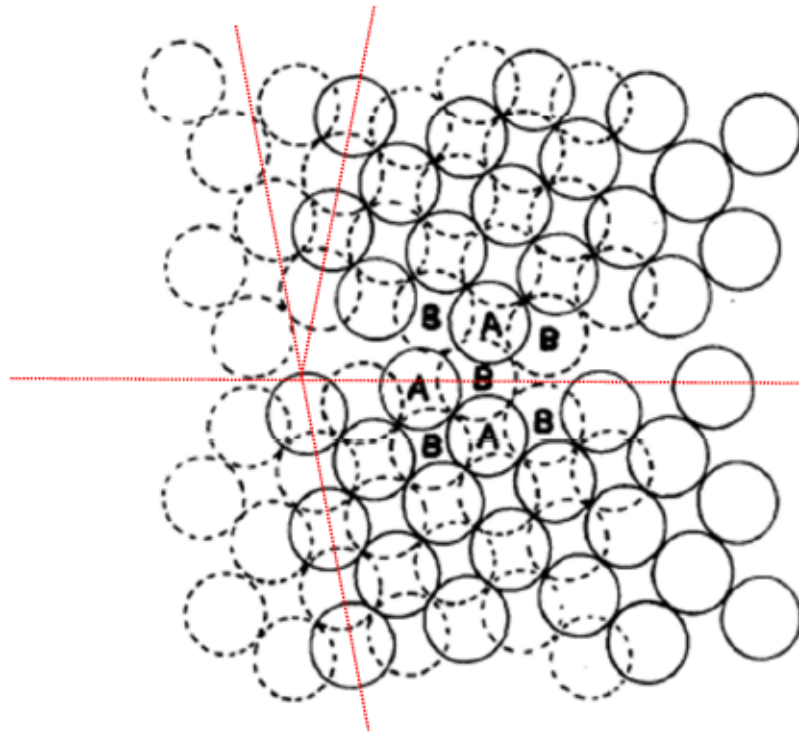
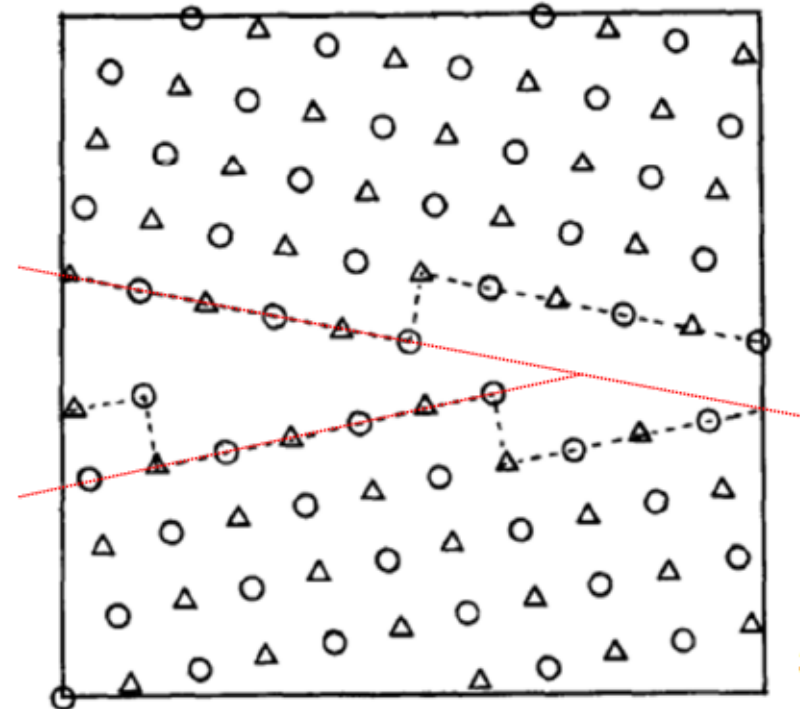
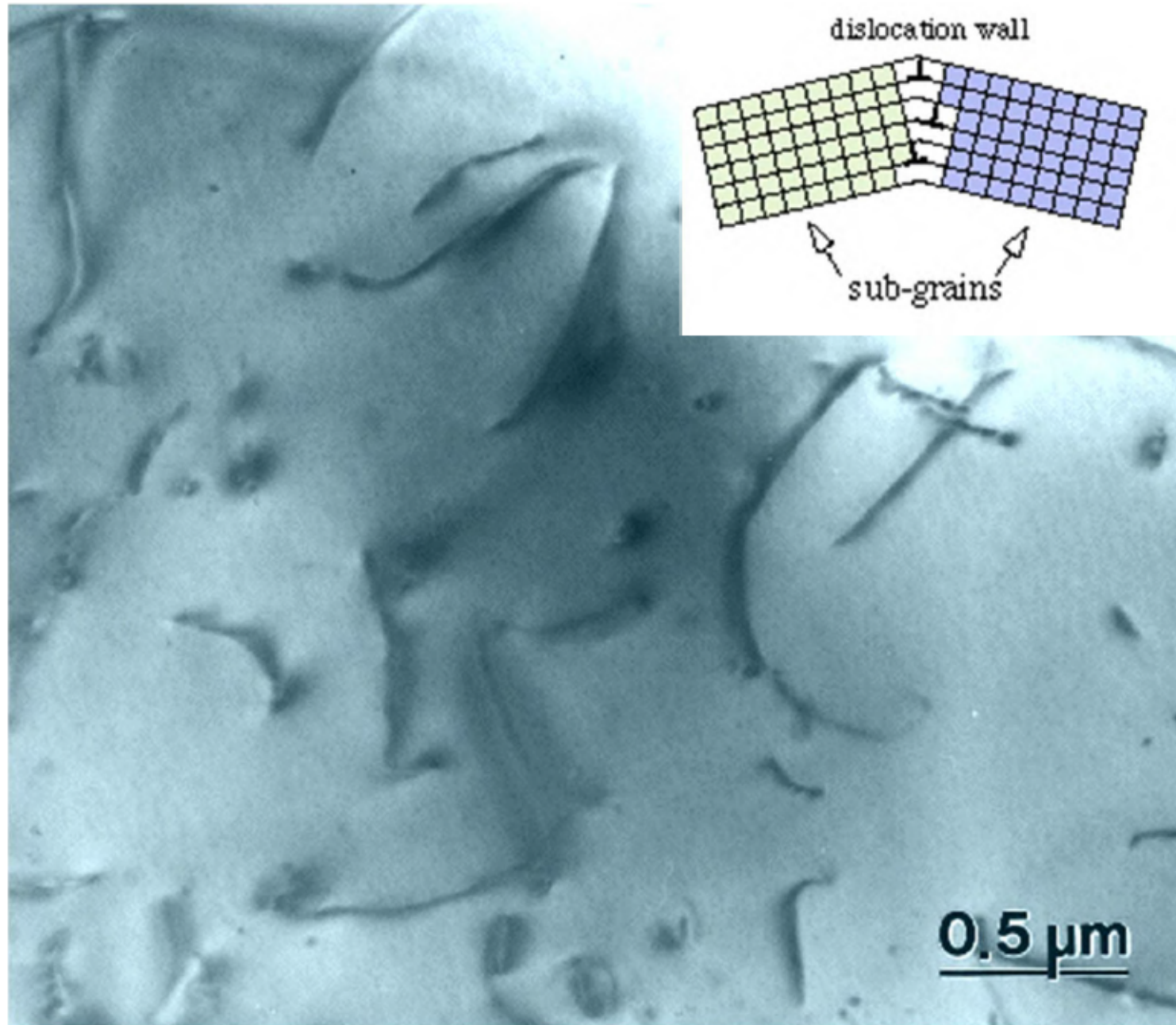


Figure 1 - 23° symmetric tilt boundary about a $\langle 001 \rangle$ axis. The circles with dashed lines represent one layer and the circles with solid lines the other layer of the AB...stacked $\{001\}$ planes. The atoms labelled A and B denote the structural unit.

Figure 2 - 23° symmetric tilt boundary about a $\langle 001 \rangle$ axis. Δ represent one layer and \circ represent the other layer of the AB..... stacked $\{001\}$ planes. The ledge like character of the boundary is shown by the dashed lines.



Dislocations



twist Boundaries

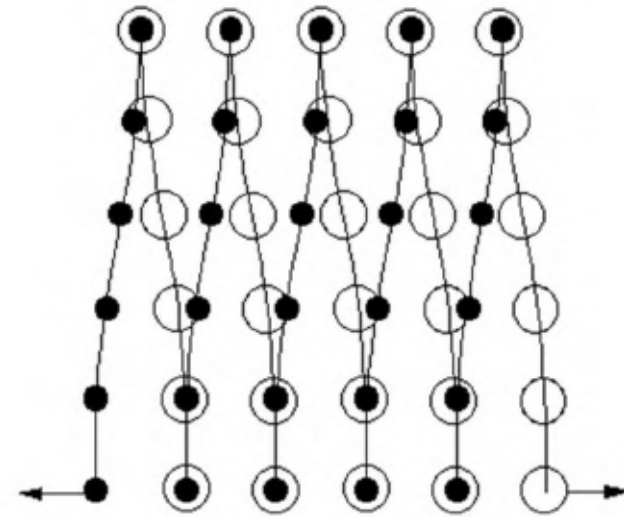
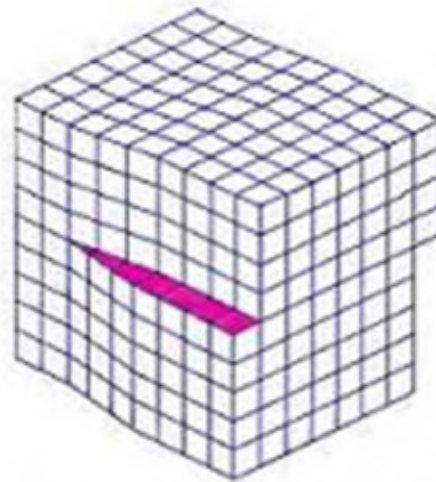
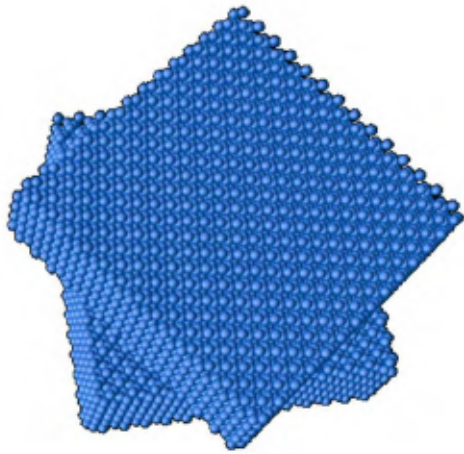
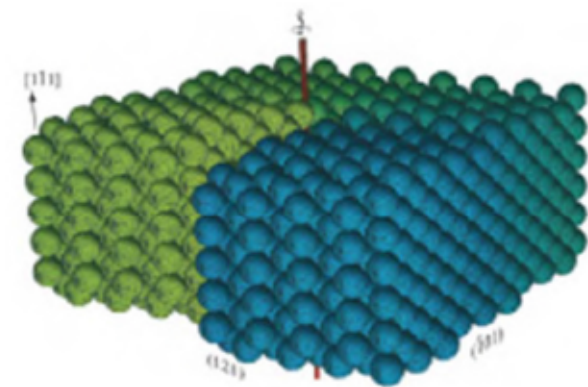
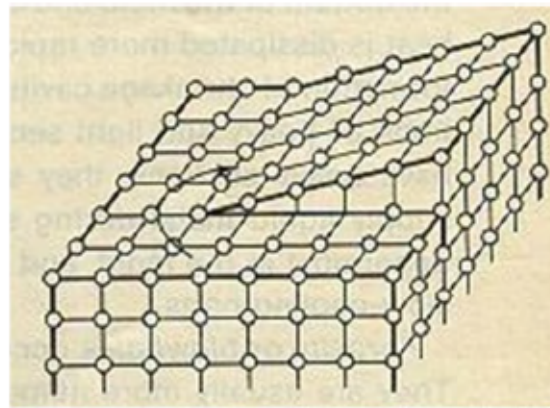
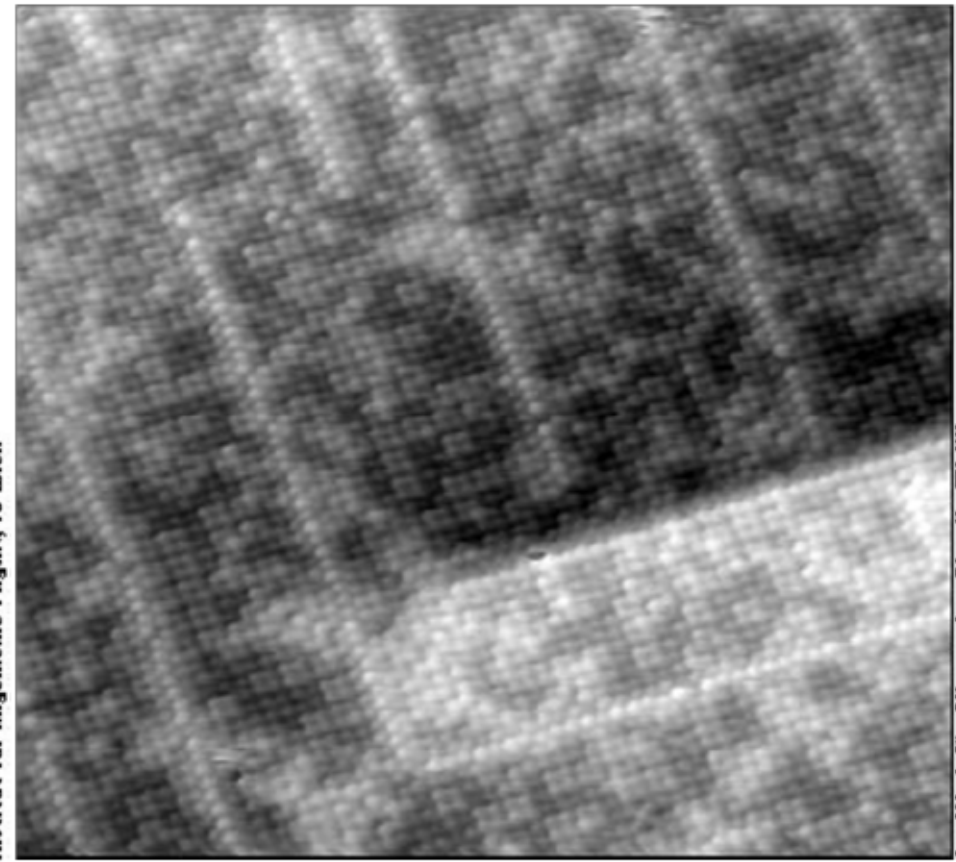
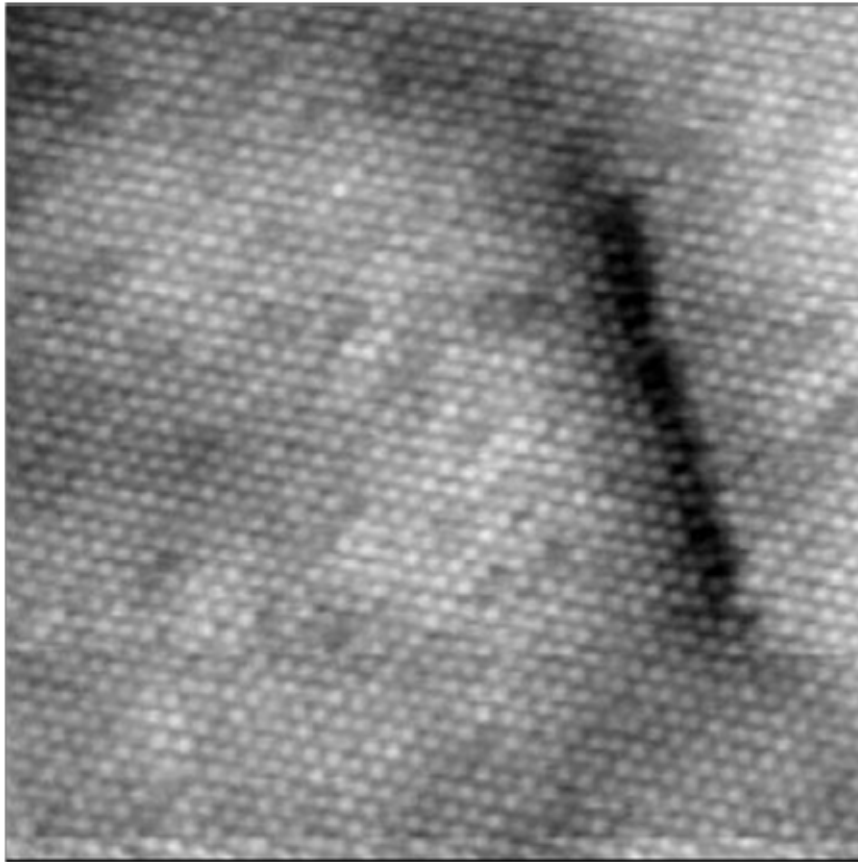


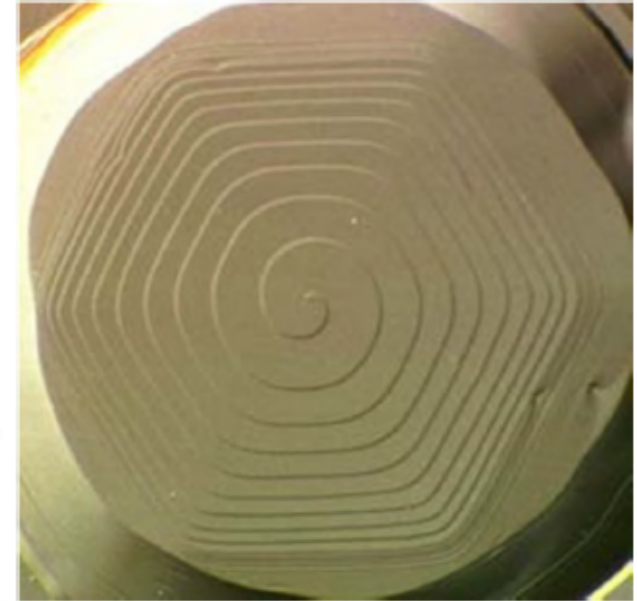
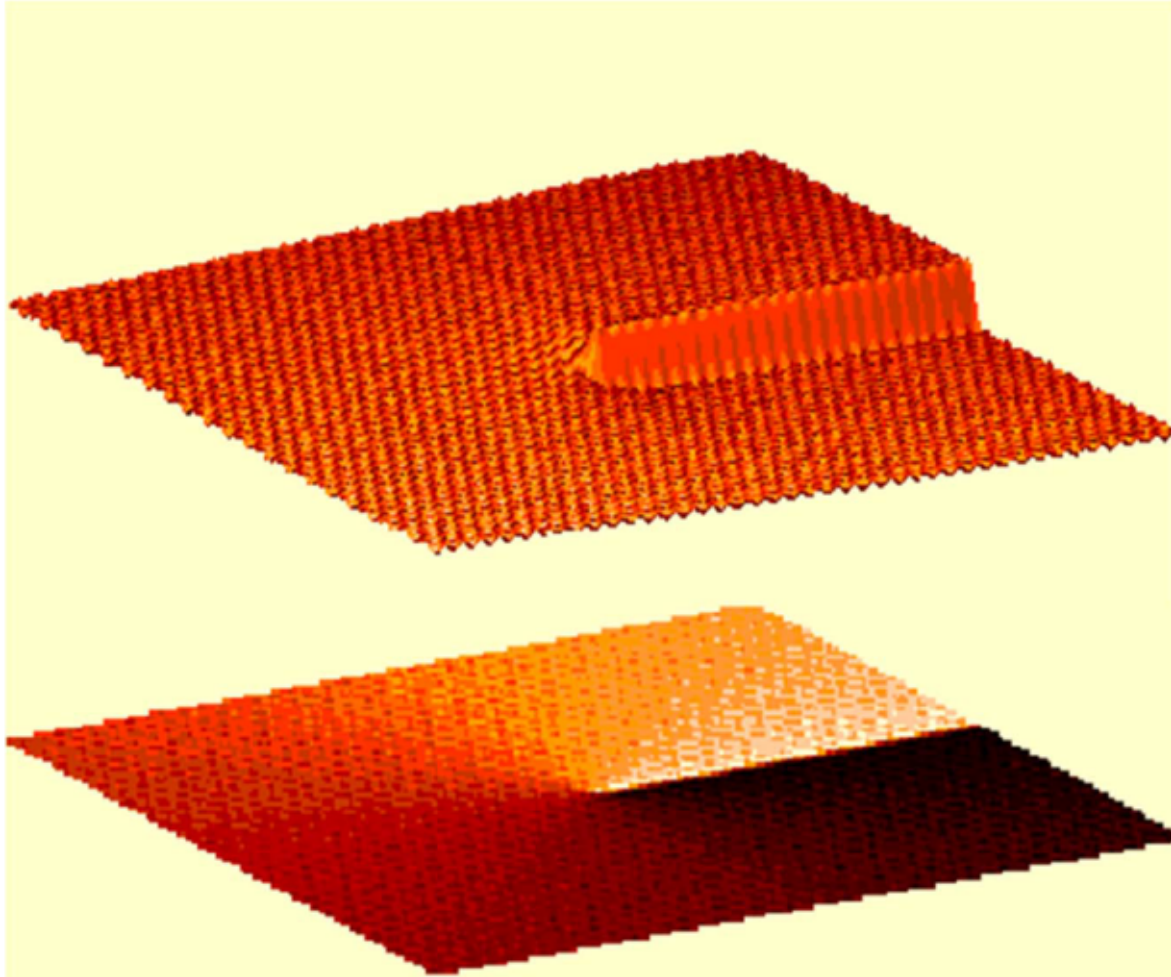
Figure 2. A screw dislocation; note the screw-like 'slip' of atoms in the upper part of the lattice



Screw dislocation



Growth of Screw dislocation



Non-symmetric Tilt Boundary

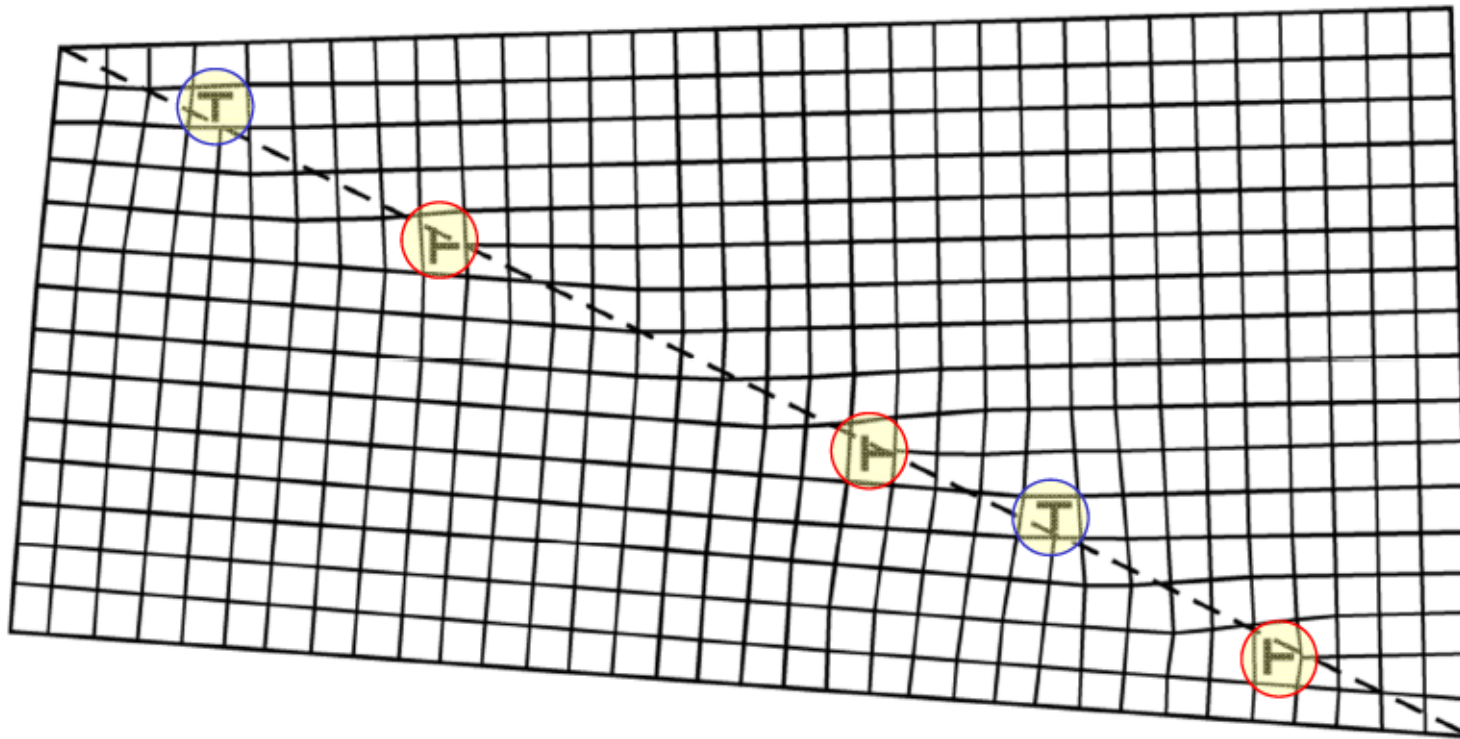


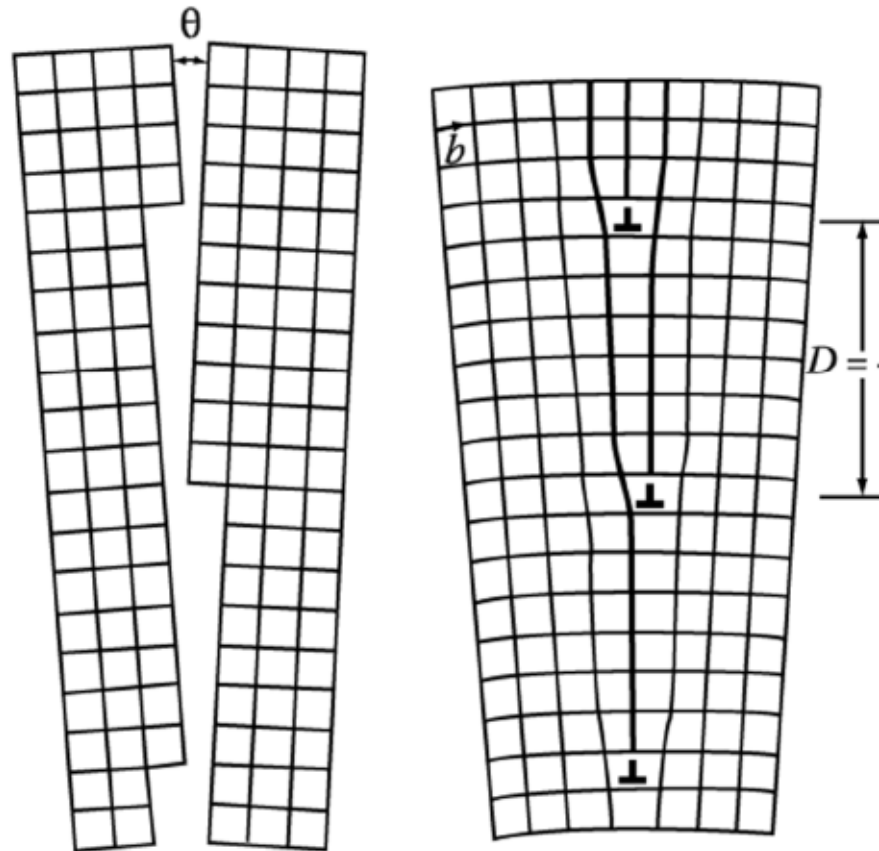
Fig. 3.8 An unsymmetrical tilt boundary. Dislocations with two different Burgers vectors are present.

If the boundary is unsymmetrical, dislocations with different burgers vectors are required to accommodate the misfit.

**In general boundaries of a mixture of the tilt and twist type,
→ several sets of different edges and screw dislocations.**

3.3.1 Low-Angle and High-Angle Boundaries

Low-Angle Tilt Boundaries



(a)

→ around edge dislocation : strain ↑

but, LATB ~ almost perfect matching

Burgers vector of the dislocations



Angular mis-orientation across the boundary

$$\sin \frac{\theta}{2} = \frac{b/2}{D}$$

$$\sin \frac{\theta}{2} \approx \frac{\theta}{2}$$

$$D \approx \frac{b}{\theta}$$

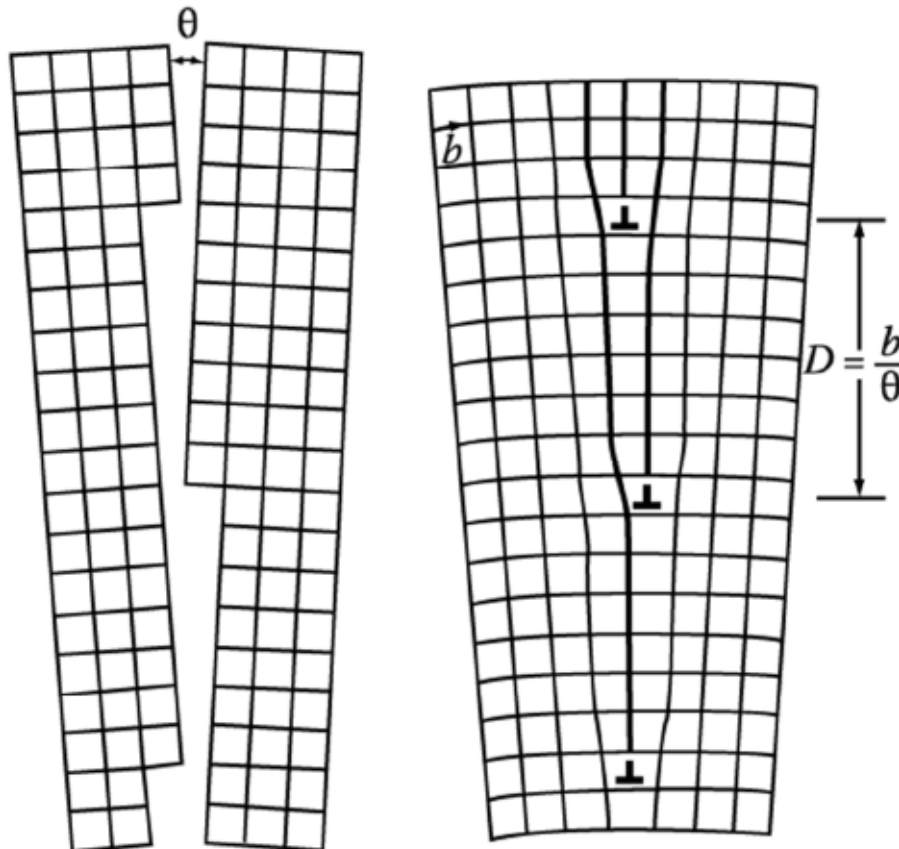
Energy of LATB ~ Total E of the dislocations within unit area of boundary

~ depends on the spacing of the dislocations (D)

(For brevity, the distinction between internal E and free E will usually not be made from now)

3.3.1 Low-Angle and High-Angle Boundaries

Low-Angle Tilt Boundaries



(a)

→ around edge dislocation : strain ↑
 but, LATB ~ almost perfect matching

→ g.b. energy : $\gamma_{g.b.} \rightarrow E / \text{unit area}$
 (energy induced from dis.)

* Relation between D and γ ?

$\sin \theta = \frac{b}{D}$, at low angle Very small $\theta \rightarrow$
 Very large D

→ $D = \frac{b}{\theta} \rightarrow \gamma_{g.b.}$ is proportional to $1/D$

→ Density of edge dislocation in low angle tilt boundary $\gamma \propto \theta$

(cf. low angle twist boundary → screw dis.)

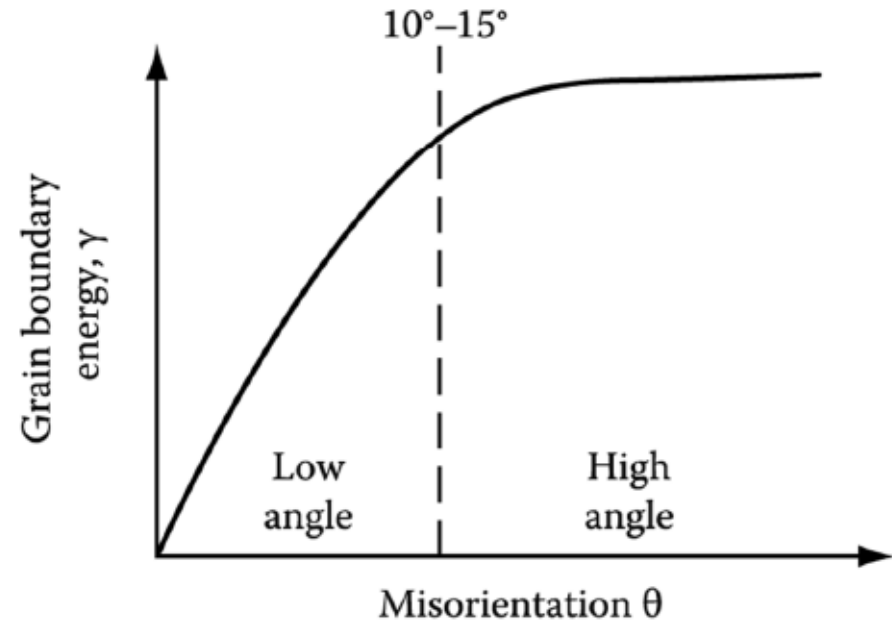
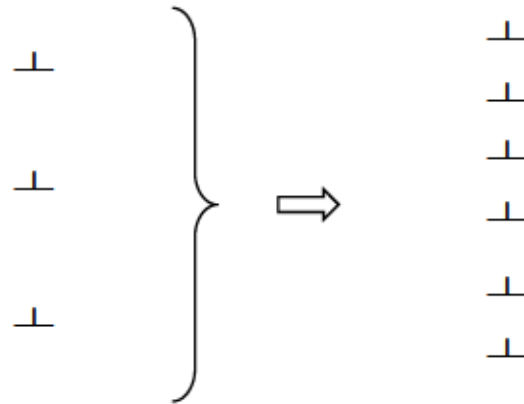
Energy of LATB ~ total energy of the dislocations within unit area of boundary

~ depends on the spacing of the dislocation (D)

Low-Angle tilt Boundaries

$$\gamma \propto \theta$$

⇒ 1) As θ increases, $\gamma_{g.b.}$ ↑



Strain field overlap
→ **cancel out**

- 2) $\gamma_{g.b.}$ increases and the increasing rate of γ ($=d\gamma/d\theta$) decreases.
- 3) if θ increases further, it is impossible to physically identify the individual dislocations
- 4) When $\theta > 10^\circ-15^\circ$, increasing rate of $\gamma_{g.b.} \sim 0$
- 5) When $\theta > 10^\circ-15^\circ$, Grain-boundary energy \sim almost independent of misorientation

Soap Bubble Model Structural difference between low-angle and high angle grain boundary

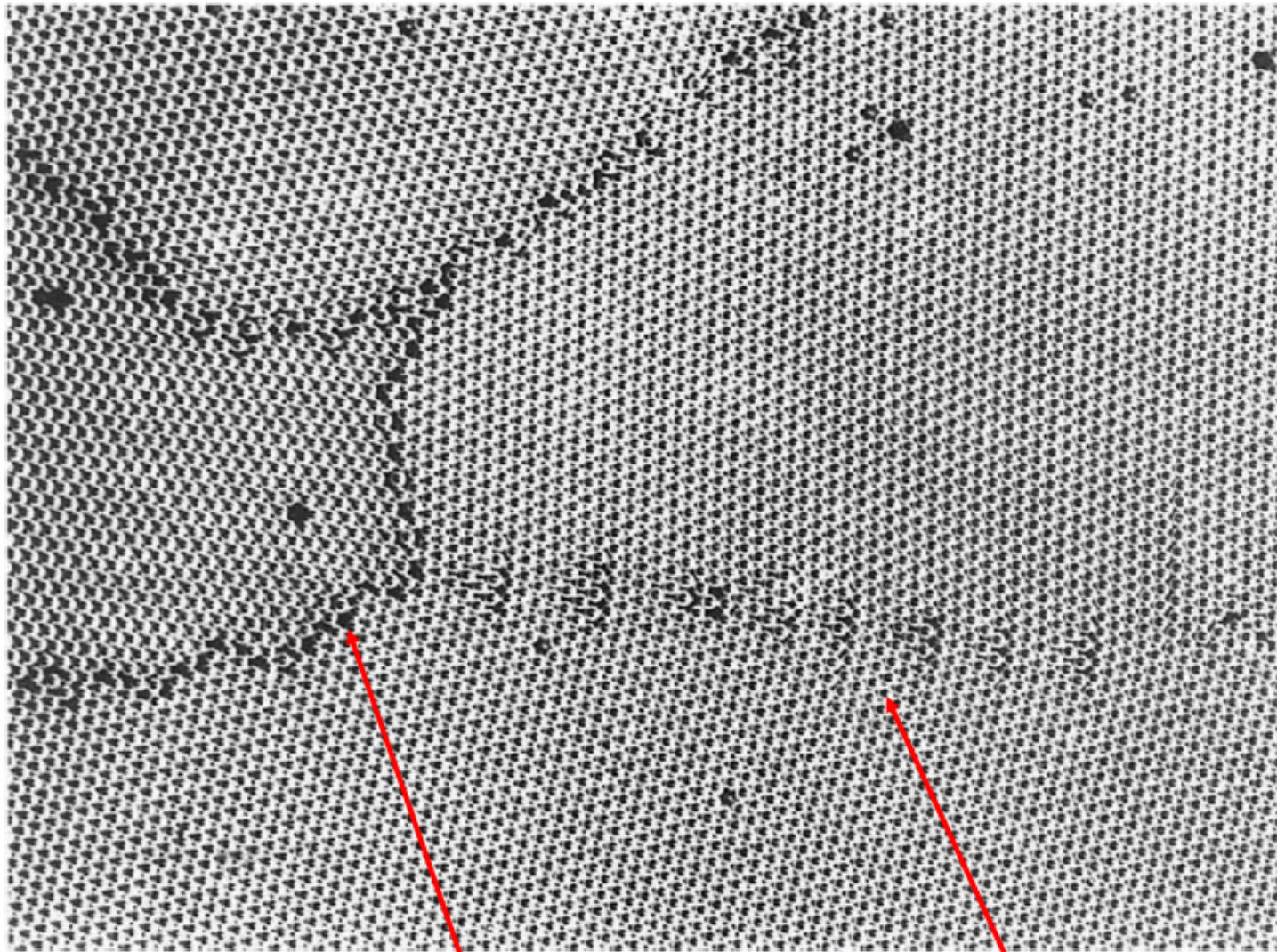


Fig. 3.11 Rafts of soap bubbles showing several grains of varying misorientation. Note that the boundary with the smallest misorientation is made up of a row of dislocations, whereas the high-angle boundaries have a disordered structure in which individual dislocations cannot be identified. *Fit very well/ very little free volume/ slightly distorted* *Large area of poor fit/relatively open structure/highly distorted*

High Angle Grain Boundary: $\theta > 10^\circ$ - 15°

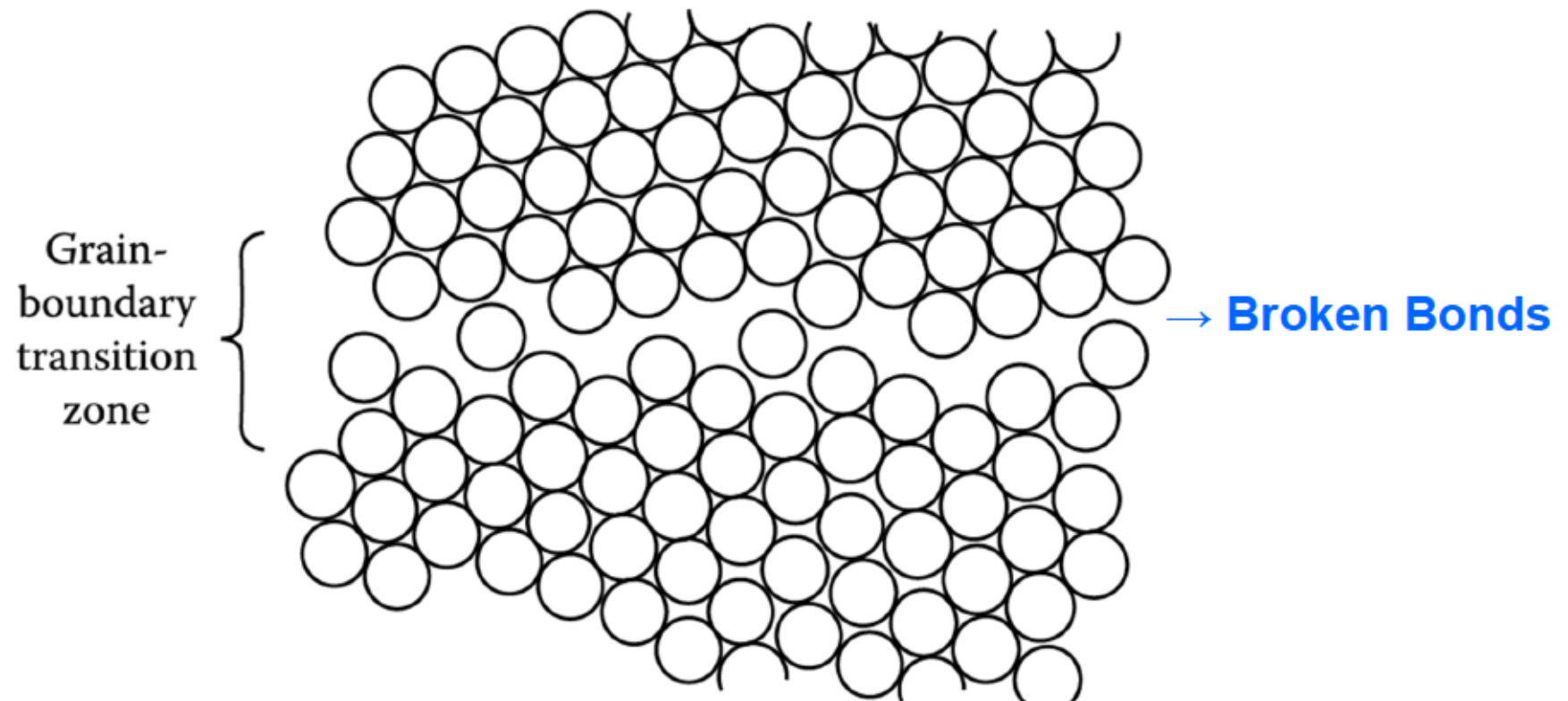


Fig. 3.10 Disordered grain boundary structure (schematic).

High angle boundaries contain large areas of poor fit and have a relatively open structure.

→ high energy, high diffusivity, high mobility (cf. gb segregation)

High Angle Grain Boundary

- Low angle boundary
 - almost perfect matching (except dislocation part)
- High angle boundary (almost)
 - open structure, large free volume

* low and high angle boundary

high angle $\gamma_{g.b.} \approx 1/3 \gamma_{sv}$ → Broken Bonds

Measured high-angle grain boundary energies

Crystal	γ (mJ m ⁻²)	T (°C)	γ_b/γ_{sv}
Sn	164	223	0.24
Al	324	450	0.30
Ag	375	950	0.33
Au	378	1000	0.27
Cu	625	925	0.36
γ -Fe	756	1350	0.40
δ -Fe	468	1450	0.23
Pt	660	1300	0.29
W	1080	2000	0.41

* As for γ_{sv} , γ_b is temperature dependent decreasing somewhat with increasing temperature.

Q: Grain boundary (α/ α interfaces)

= Boundaries in Single-Phase Solids

(a) Low-Angle and High-Angle Boundaries

(b) Special High-Angle Grain Boundaries

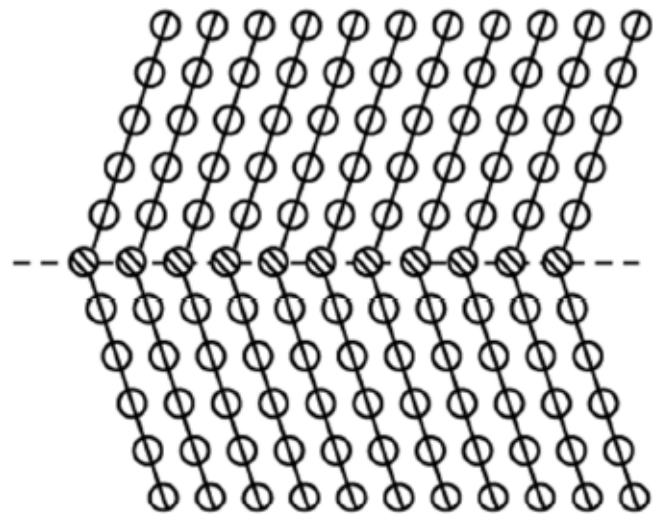
(c) Equilibrium in Polycrystalline Materials

Boundaries in Single-Phase Solids

(a) Low-Angle and High-Angle Boundaries

(b) Special High-Angle Grain Boundaries I

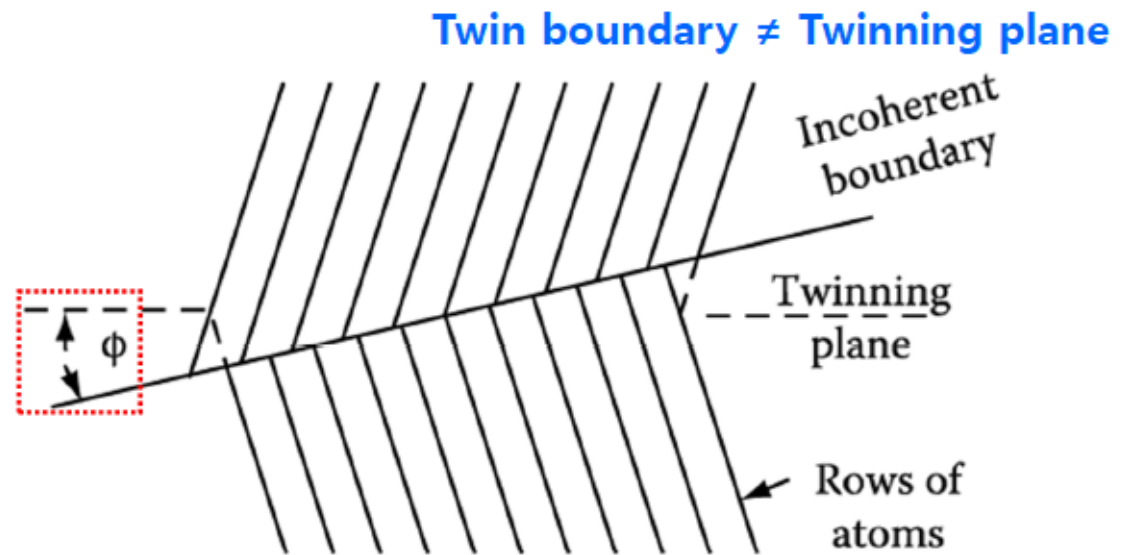
: high angle boundary but with low $\gamma_{g.b.}$



a) **Coherent twin boundary**
symmetric twin boundary

→ low $\gamma_{g.b.}$

Atoms in the boundary
are essentially in
undistorted positions

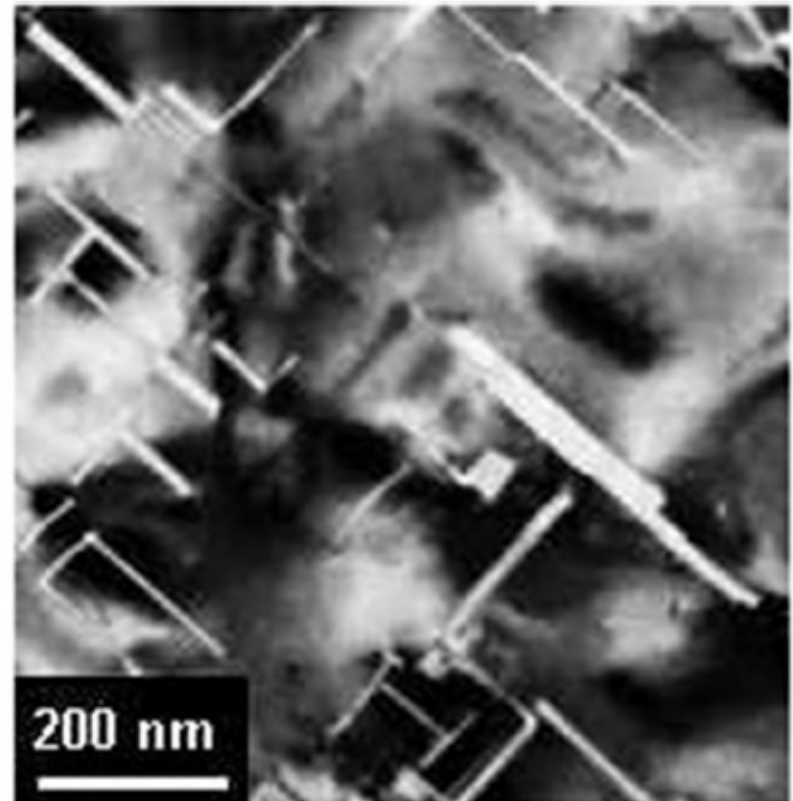
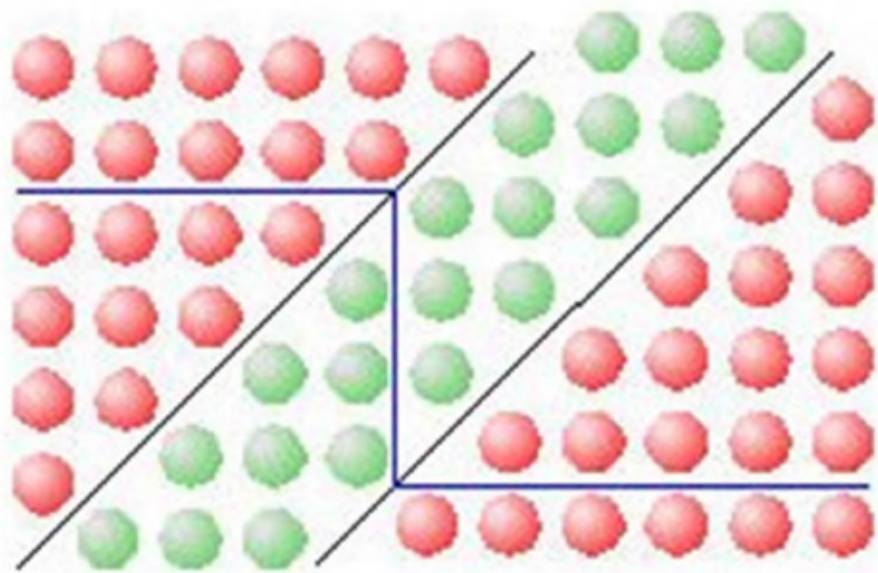


b) **Incoherent twin boundary**
asymmetric twin boundary

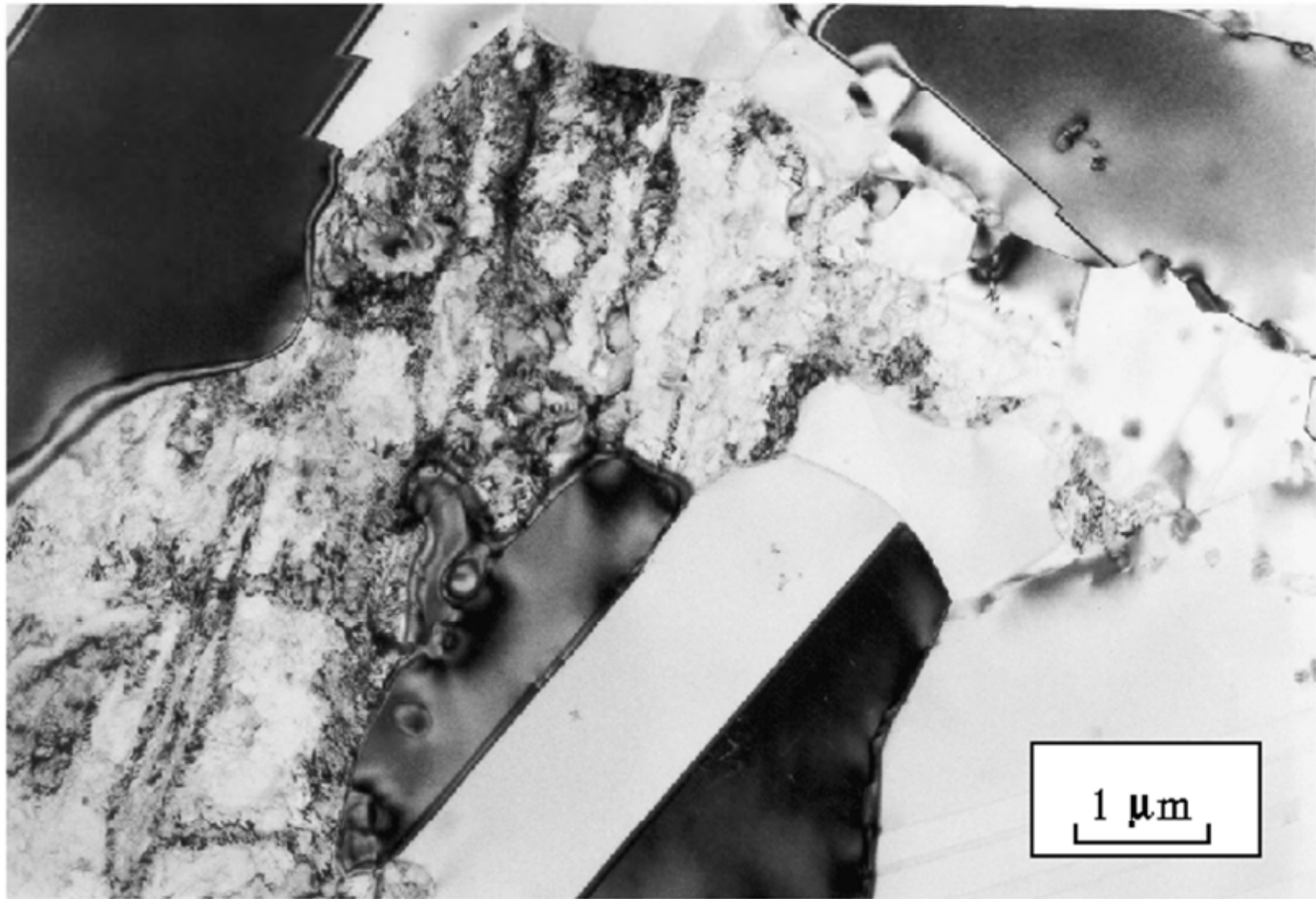
→ low $\gamma_{g.b.}$

Energy of twin boundary ~
very sensitive to the orientation
of the boundary plane

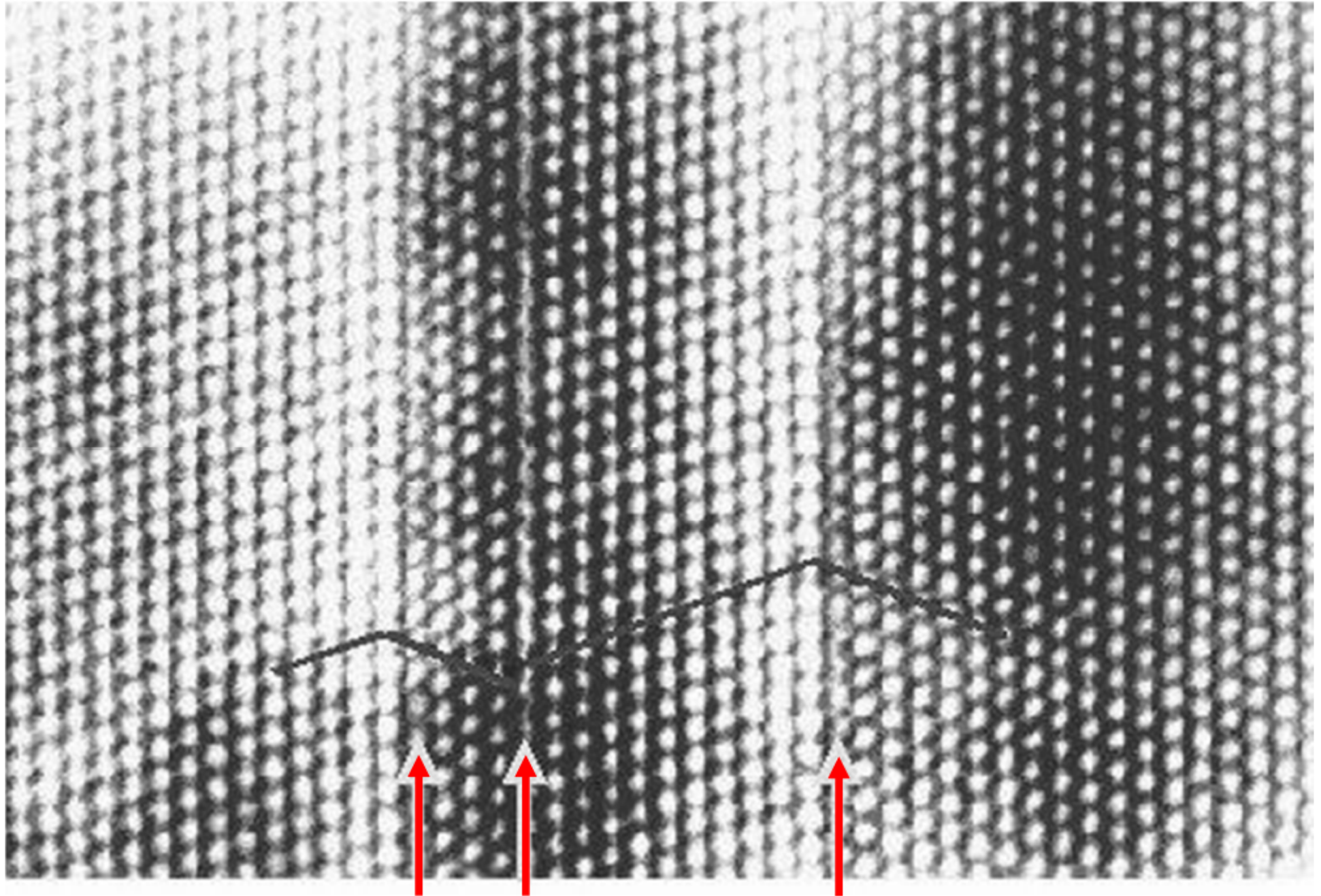
Twin boundary



Twin boundary



Twin boundary



(b) Special High-Angle Grain Boundaries I

c) Twin boundary energy as a function of the grain boundary orientation

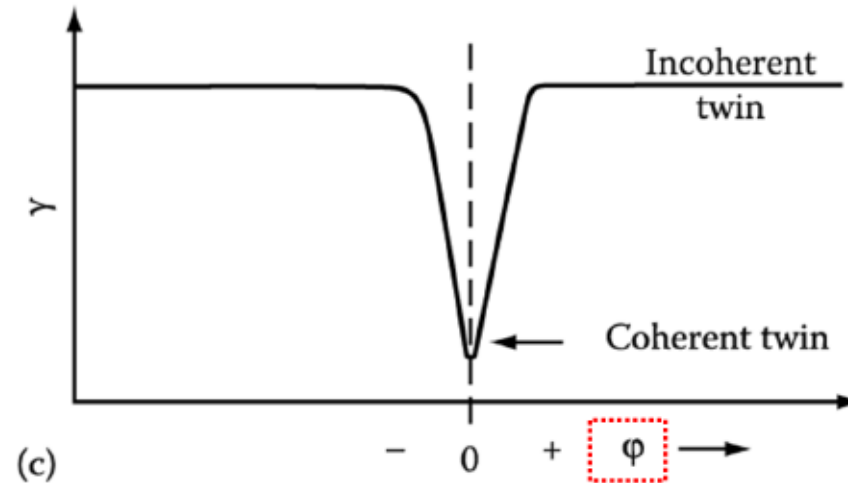


Table 3.3 Measured Boundary Free Energies for Crystals in Twin Relationships
(Units mJ/m^2)

Crystal	Coherent Twin-Boundary Energy	Incoherent Twin-Boundary Energy	Grain-Boundary Energy
Cu	21	498	623
Ag	8	\ll	377
Fe-Cr-Ni (stainless steel type 304)	19	209	835

(b) Special High-Angle Grain Boundaries II

Two grains ~ a rotation about a (100) axis < a rotation about a (110) axis

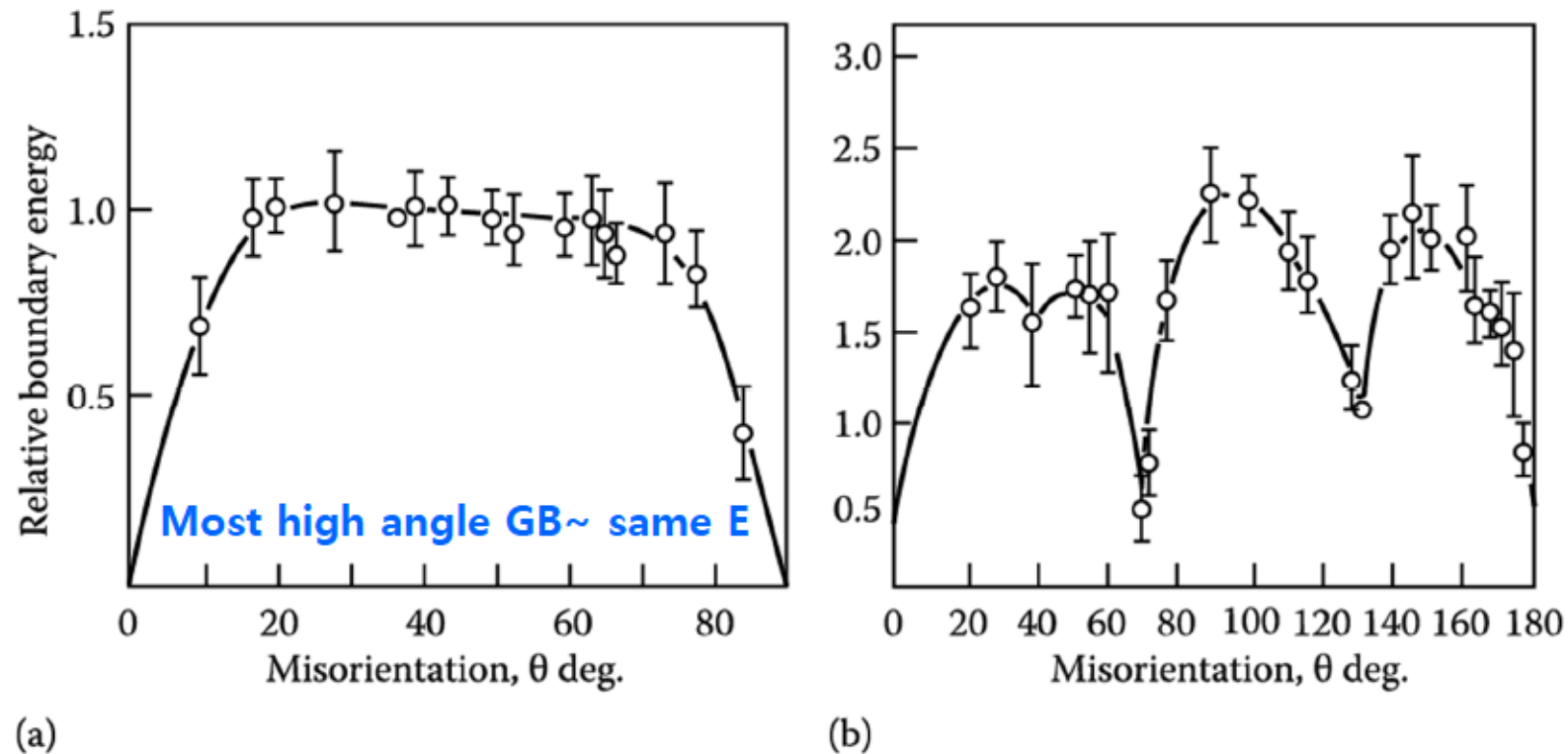


Fig. 3.13 Measured grain boundary energies for symmetric tilt boundaries in Al (a) When the rotation axis is parallel to (100), (b) when the rotation axis is parallel to (110).

Why are there cusps in Fig. 3.13 (b)?

In FCC metal, several large-angle orientations with significantly lower energies than the random boundaries.

$\phi = 70.5^\circ$ ~ coherent twin boundary (next page), others ~ not well understood

- symmetrical tilt boundary
~38.2 °
- a small group of atoms are repeated regular intervals along the boundary.
~relatively little free volume

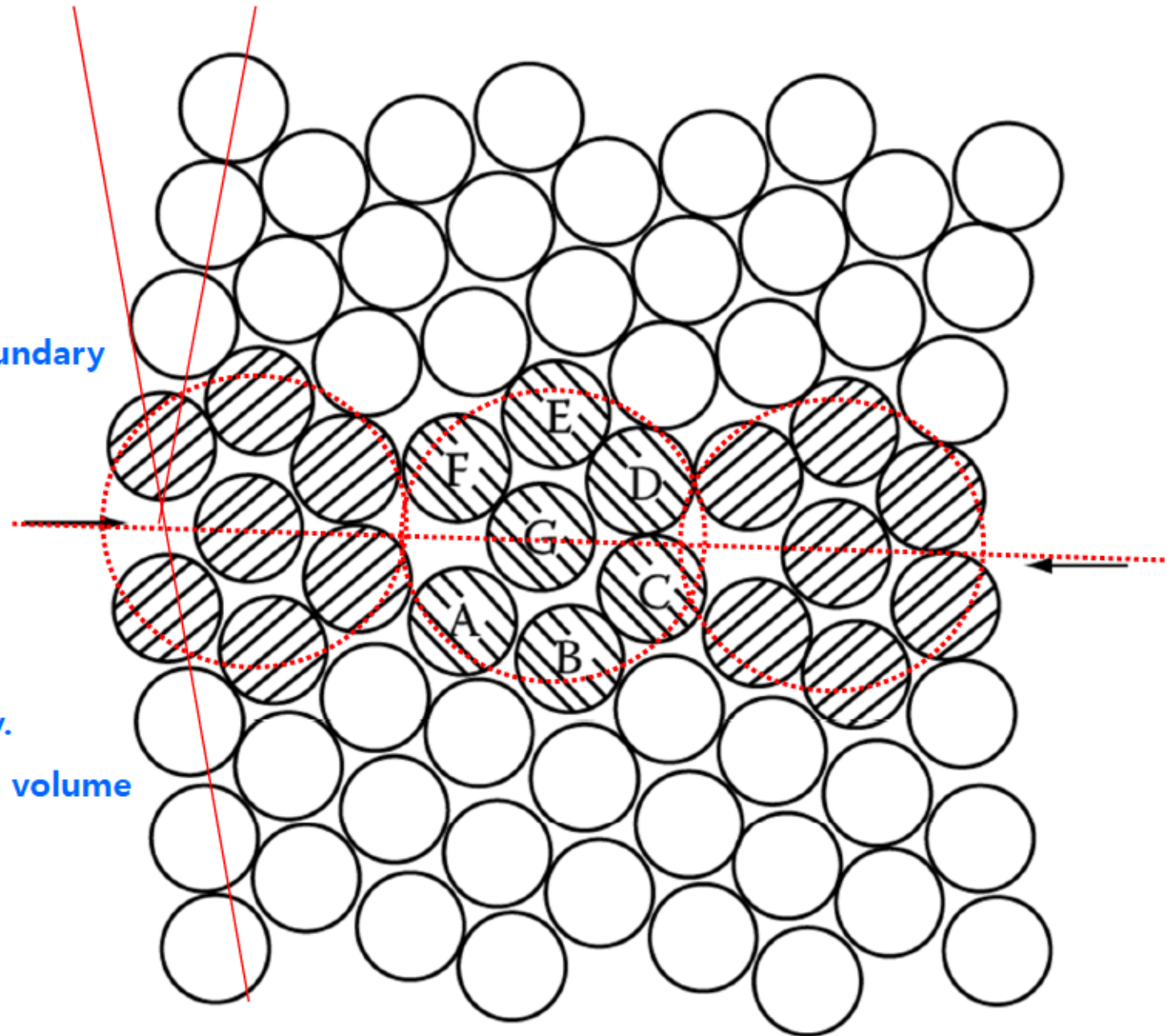


Fig. 3. 14 Special grain boundary: two dimensional example.

입계의 원자구조가 주위의 격자와 똑넓게 잘 일치 됨

Contents for previous class

3) Boundaries in Single-Phase Solids

(a) Low-Angle and High-Angle Boundaries

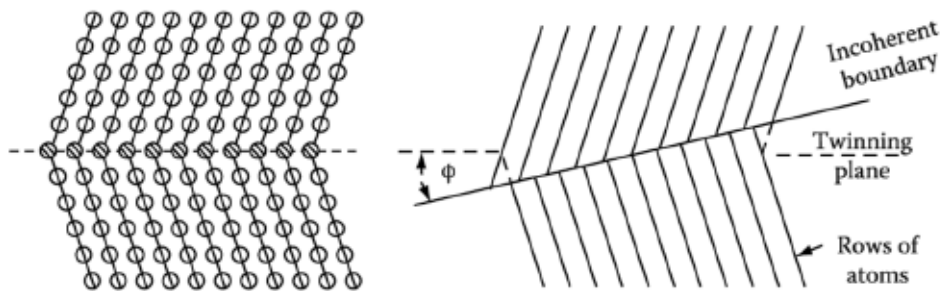
$\Theta < 15^\circ$: total energy of the dislocations within unit area of boundary

$\Theta > 15^\circ$: impossible to physically identify the individual dislocations \rightarrow strain field overlap \rightarrow cancel out

Broken Bonds \rightarrow high angle $\gamma_{g.b.} \approx 1/3 \gamma_{SN}$.

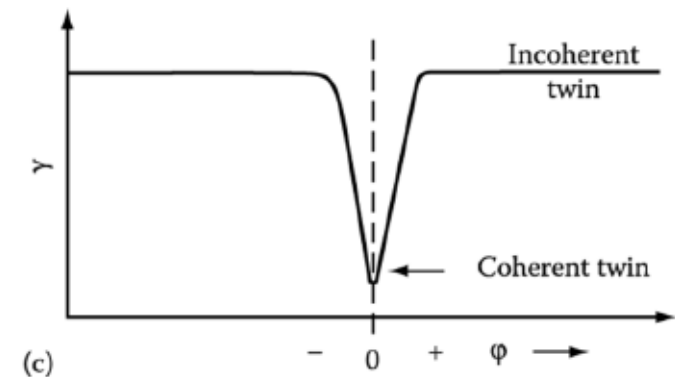
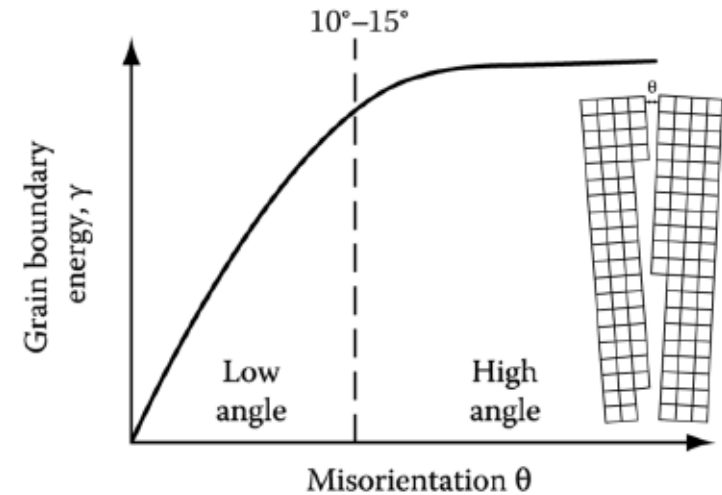
(b) Special High-Angle Grain Boundaries

: high angle boundary but with low $\gamma_{g.b.}$



\rightarrow twin boundary

Atoms in the boundary are essentially in undistorted positions \sim relatively little free volume



Contents for today's class

< Boundaries in Single-Phase Solids >

(c) Equilibrium in Polycrystalline Materials

1) GB intersection: Balance of 1) boundary E & 2) surface tension

GBs in a polycrystal can adjust themselves during annealing to produce a metastable equilibrium at the GB intersections.

2) Thermally Activated Migration of Grain Boundaries

- Grain coarsening at high T, annealing due to metastable equilibrium of GB

3) Kinetics of Grain Growth

- Grain boundary migration by thermally activated atomic jump

- Mobility of GB ~ GB structures and GB segregations

i.e Normal grain growth \longleftrightarrow Abnormal grain growth

4) Effect of second-phase particle on GB migration: Zener Pinning

$$\bar{D}_{\max} = \frac{4r}{3f_v}$$

Q: Grain boundary (α/α interfaces)

= Boundaries in Single-Phase Solids

(a) Low-Angle and High-Angle Boundaries

(b) Special High-Angle Grain Boundaries

(c) Equilibrium in Polycrystalline Materials

1) GB intersection: Balance of 1) boundary E & 2) surface tension

GBs in a polycrystal can adjust themselves during annealing to produce a metastable equilibrium at the GB intersections.

(c) Equilibrium in Polycrystalline Materials

Microstructure → determined by how the different GBs join together in space

⇒ Examine how the possibility of different GB energies affects the microstructure of a poly crystalline material

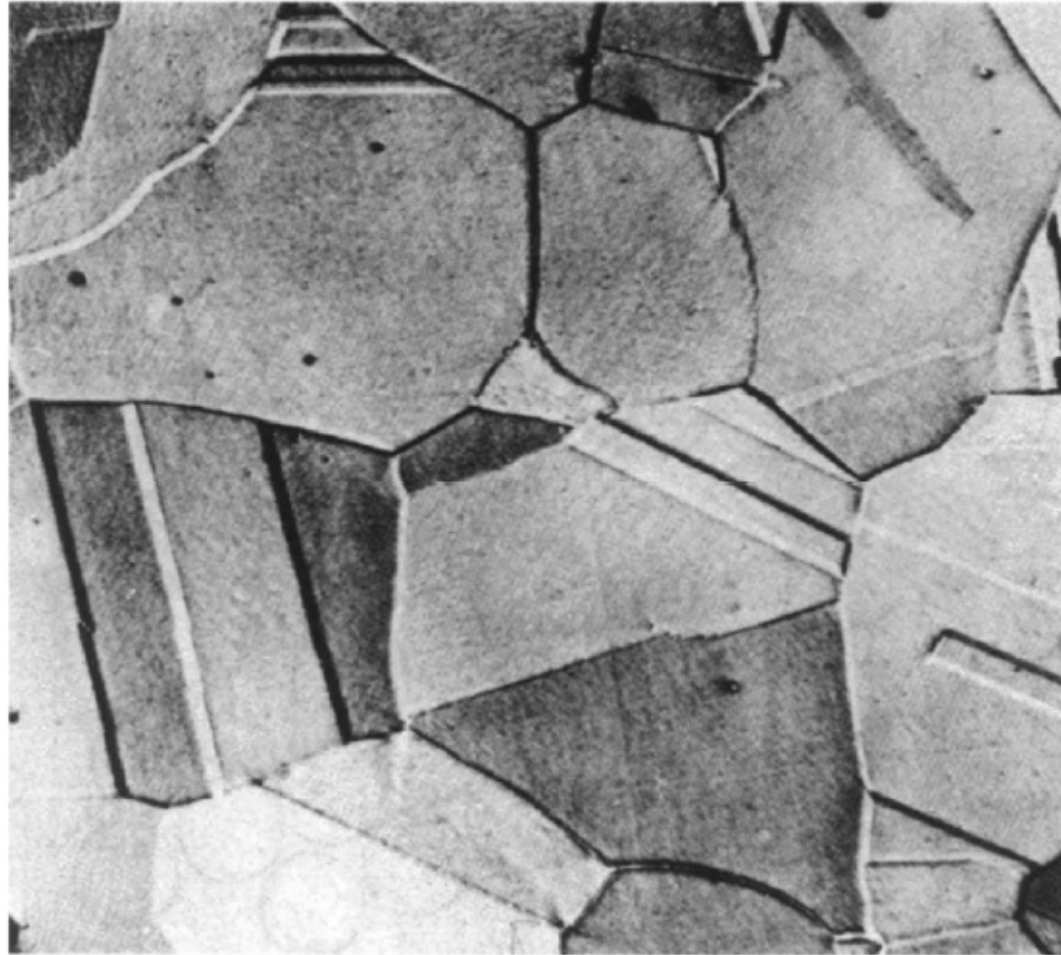
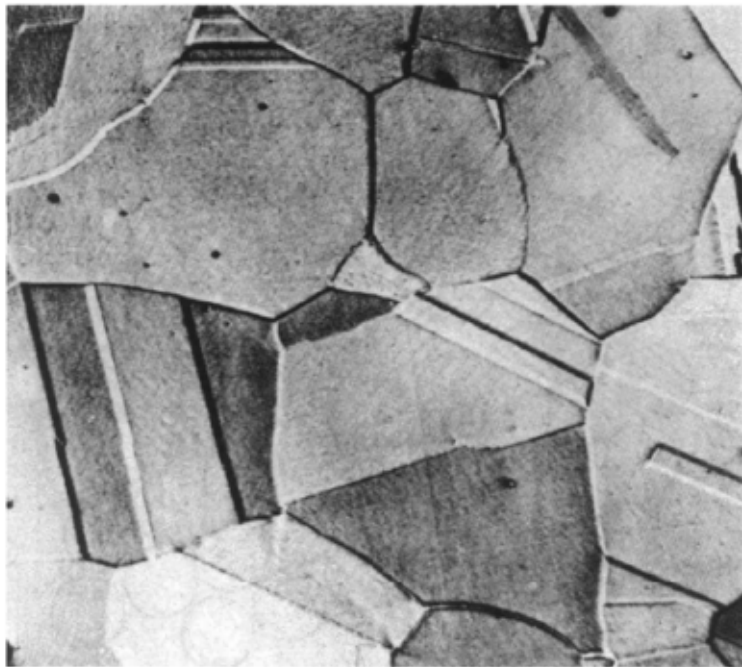


Fig. 3.15 Microstructure of an annealed crystal of austenitic stainless steel. 36
: contains high-/low-angle GBs as well as (in-)coherent twin Bs with different GB energies

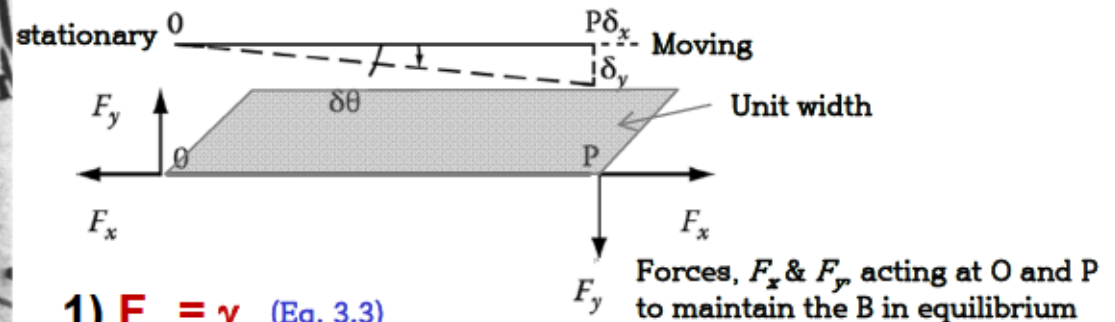
Poly grain material: consider the factors that control the grain shapes!

Two grains: a plane (GB), three grains: a line (grain edge), four grains: at a point (grain corner)



2) Conditions for equilibrium at a GB junction

by considering the forces that each B exerts on the junction



1) $F_x = \gamma$ (Eq. 3.3)

2) F_y ?

P is moved at a small distance (δ_y)

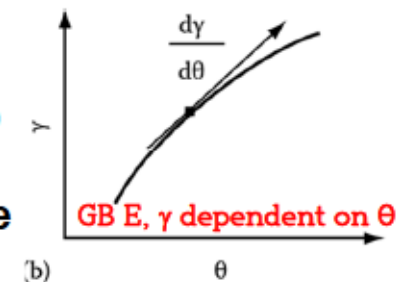
A. work done by : $F_y \delta_y$

B. increase boundary energy caused

by the change in orientation $\delta\theta \sim l (d\gamma/d\theta) \delta\theta$

$F_y \delta_y = l (d\gamma/d\theta) \delta\theta$ ($\because \delta_y \sim l d\theta$)

$\rightarrow F_y = d\gamma/d\theta$ torque force



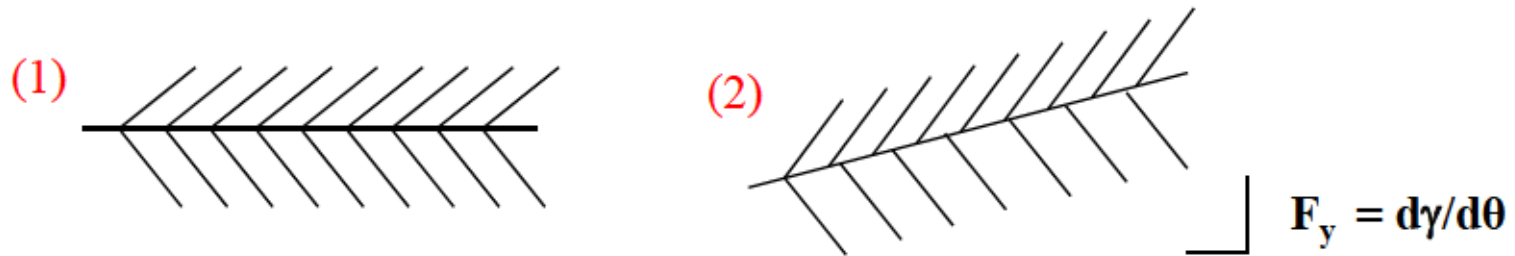
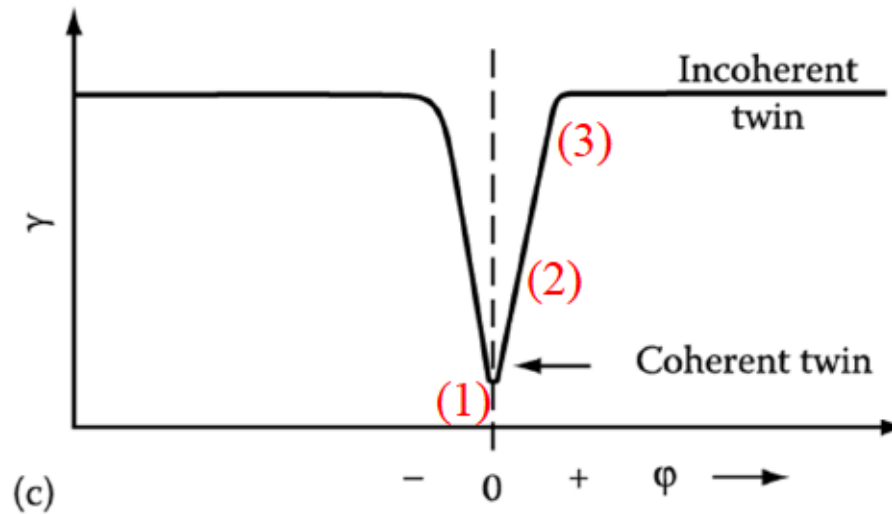
1) Why GBs exist at all in annealed materials?

Equilibrium ~ Mater. with no GB

\because G.B.=high-E regions $\rightarrow G \uparrow$

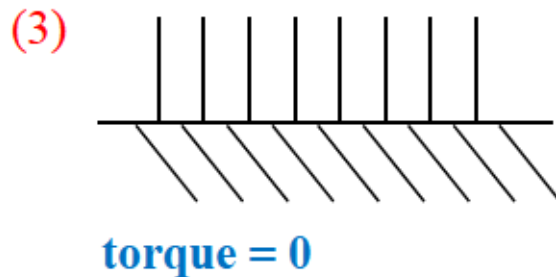
: never a true equilibrium structure

\rightarrow GBs in a polycrystal can adjust themselves during annealing to produce a metastable equilibrium at the GB intersections.



Minimum $\gamma \sim \text{torque} = 0$ No rotation!

If Pulling force, $F_y > (d\gamma/d\theta)_{\text{cusp}} \rightarrow \text{Rotating}$



\rightarrow There is little effect of orientation

$F_y = d\gamma/d\theta \sim \text{torque} > 0$

If the GB E is dependent on the orientation of the B, a force $d\gamma/d\theta (>0)$ must be applied to the ends of the boundary to prevent it rotating into a lower energy orientation.

입계 E가 입계 방위에 의존한다면, 회전하지 않고 유지하기 위해 입계에 cusp까지 끌어당기는 힘에 대응하는 힘 작용

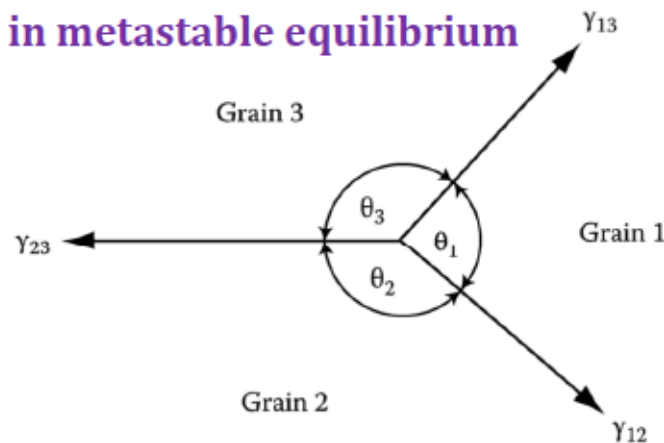
\Rightarrow How metastable equilibrium? \rightarrow force (torque)

If the boundary E is independent of orientation,

* **General high angle boundary** : $d\gamma/d\theta \approx 0$ (GB behaves like a soap film)

→ Under these conditions the requirements for metastable equilibrium at junction between three grains is that the boundary tensions $\gamma_{13}, \gamma_{23}, \gamma_{12}$ must balance.

3) **The balance of GB tensions for a GB intersection in metastable equilibrium**



$$\frac{\gamma_{23}}{\sin \theta_1} = \frac{\gamma_{31}}{\sin \theta_2} = \frac{\gamma_{12}}{\sin \theta_3} \quad (\text{Eq. 3.13})$$

if all GBs have same GB energy independent of boundary orientation

$$\rightarrow \theta = 120^\circ$$

Eq. 3.13 applies to any three boundaries
i.e. grain 1 ~ different phase to grain 2 & 3.

Ex) If the solid-vapor energy (γ_{sv}) is the same for both grains,

$$2\gamma_{sv} \cos \frac{\theta}{2} = \gamma_b$$

(Here, presence of any torque terms ~ neglected)

One method of measuring GB energy:

: anneal a specimen at a high temp. and then measure the angle at the intersection of the surface with B.

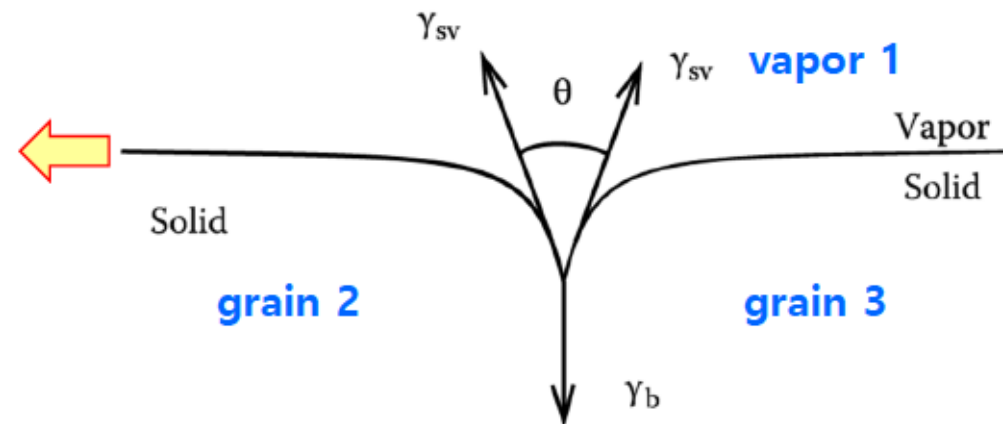


Fig. 3. 18 The balance of surface and grain boundary tensions at the intersection of a grain boundary with a free surface.

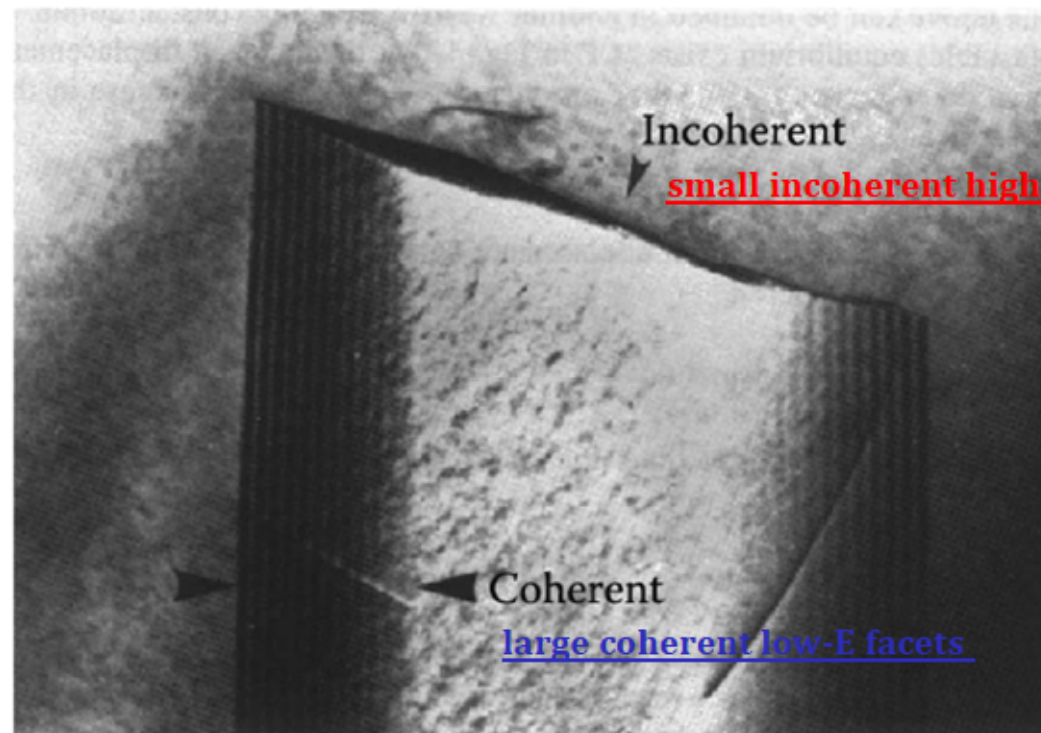
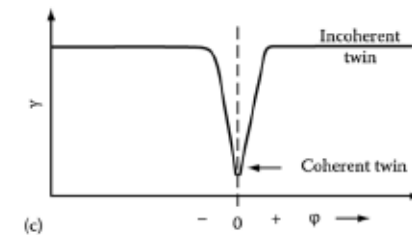
* **Junction between coherent and incoherent twin boundary segments showing the importance of torque effects**

: the orientation dependence of twin boundary E, Fig. 3.13b

→ It is energetically favorable for twin boundaries to align themselves parallel to the twinning plane.

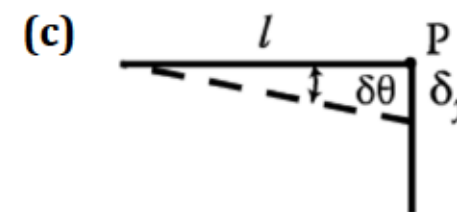
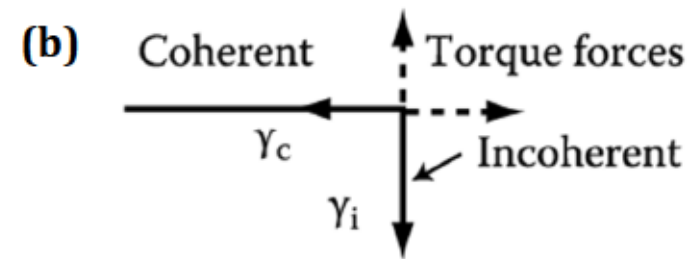
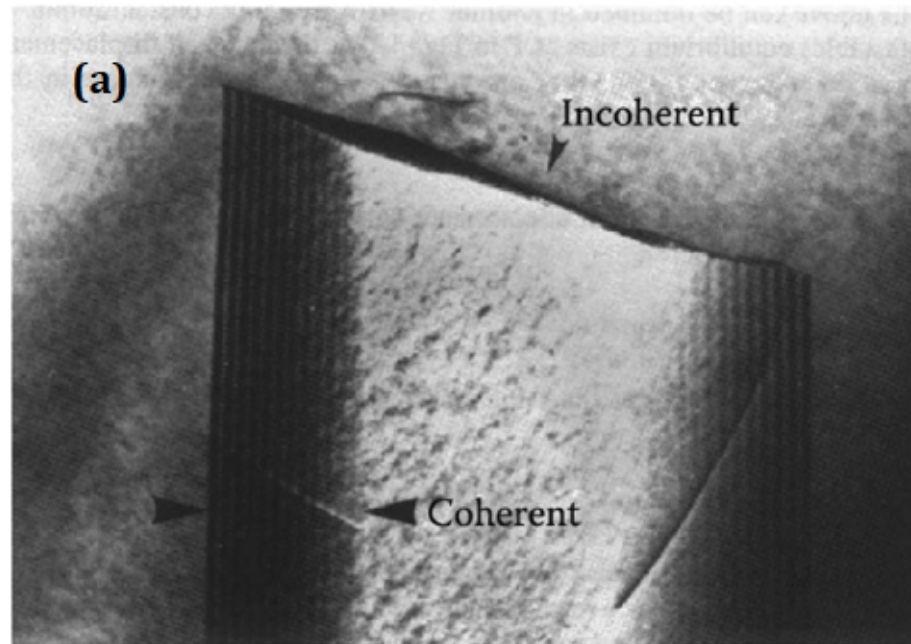
→ If the boundary is constrained to follow a macroscopic plane that is near but not exactly parallel to the twinning plane the boundary will usually develop a stepped appearance with large coherent low-E facets and small incoherent high-E risers.

→ does not minimize the total twin boundary E but minimize the total free E



(a) twin boundary in a thin foil specimen as imaged in the TEM

*** Junction between coherent and incoherent twin boundary segments showing the importance of torque effects**



(a) twin B in a thin foil specimen as imaged in the TEM, (b) & (c), the coherent and incoherent segments of the twin B.

At the coherent/incoherent twin junction as shown in (b),

incoherent twin B tension, γ_i must be balanced by a torque term

$$\gamma_i \leq d\gamma_c/d\theta$$

Likewise, coherent twin B tension, γ_c must be balanced by a torque term

$$\gamma_c \leq d\gamma_i/d\theta$$

However, since γ_c is usually very small, the incoherent interface need only lie in a rather shallow energy cusp.

From energy consideration,

if (metastable) equilibrium exists at P in Fig. (c), then a small displacement such as that shown should either produce no change or an increase in the total free energy of the system, i.e. $dG > 0$

considering unit depth a small displacement δy at P will increase the total free E by an amount

$$dG = l (d\gamma_c/d\theta) \delta\theta - \gamma_i \delta y > 0 \quad (\because \delta y \sim l d\theta) \quad \Rightarrow \quad \gamma_i \leq d\gamma_c/d\theta$$

Q: Grain boundary (α/α interfaces)

= Boundaries in Single-Phase Solids

(a) Low-Angle and High-Angle Boundaries

(b) Special High-Angle Grain Boundaries

(c) Equilibrium in Polycrystalline Materials

2) Thermally Activated Migration of Grain Boundaries

: Grain coarsening at high T, annealing due to metastable equilibrium of GB

Considering factors of G.B. growth

(a) Pinning particle

(b) 2nd phases

(c) Anisotropic σ , M

(d) Impurity (solute) drag

(e) Strain energy

(f) Free surface

GB intersection: Balance of 1) boundary E & 2) surface tension

3.3.4. Thermally Activated Migration of Grain Boundaries

If the boundary is curved in the shape of cylinder, Fig. 3.20a, it is acted on by a force of magnitude γ/r towards its center of curvature.

Therefore, the only way the boundary tension forces can balance in three dimensions is if the boundary is planar ($r = \infty$) or if it is curved with equal radii in opposite directions, Fig. 3.20b and c.

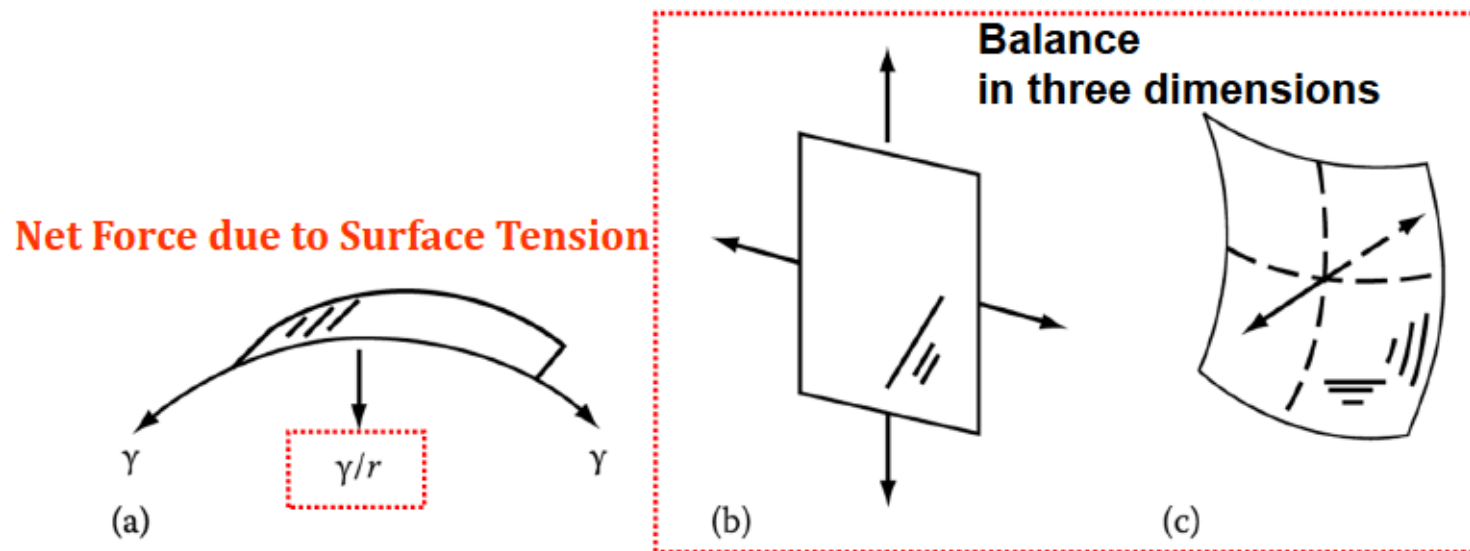


Fig. 3. 20 (a) A cylindrical boundary with a radius of curvature r is acted on by a force γ/r . (b) A planar boundary with no net force. (c) A doubly curved boundary with no net force.

A random grain structure is inherently unstable and, on annealing at high temperatures, the unbalanced forces will cause the boundaries to migrate towards their centers of curvature.

a) Direction of Grain Boundary Migration during Grain Growth

For isotropic grain boundary energy in two dimensions,

Equilibrium angle at each boundary junction? → 120° 3 boundaries intersections

Equilibrium angle at each boundary junction in 3D? → $109^\circ 28'$ A corner formed by 4 grains

Morphology of metastable equilibrium state → Migration during annealing

Effect of different boundary curvatures in two dimensions

Boundaries around Grain < 6
; grain shrink, disappear

Boundaries around Grain = 6
; equilibrium

Boundaries around Grain > 6
; grain growth

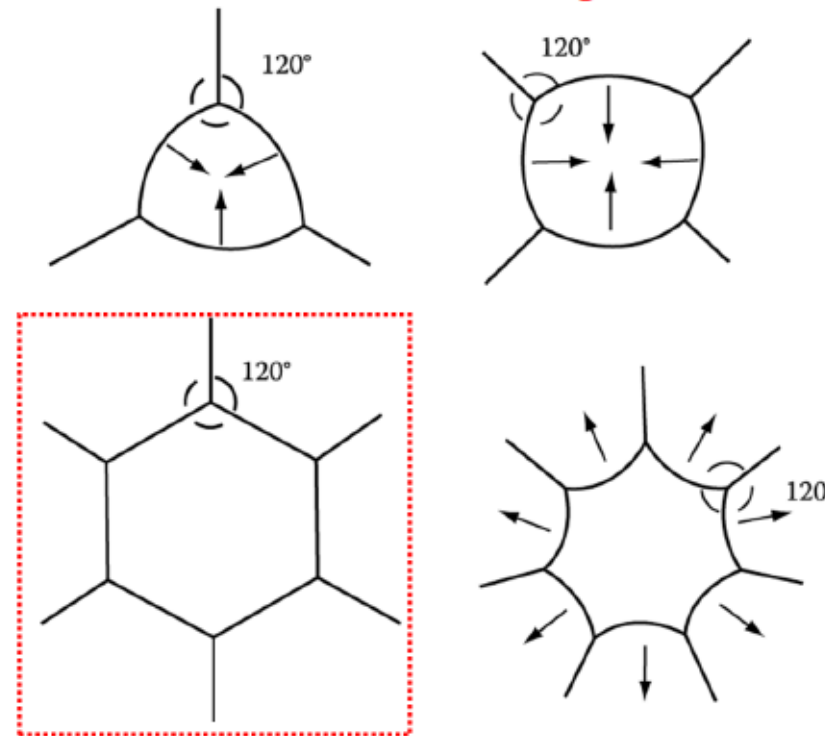


Fig. 3. 21 Two-dimensional GB configurations, The arrows indicate the directions boundaries will migrate during grain growth.

⇒ Reduce the # of grains, increase the mean grain size, reducing the total G.B. energy called **grain growth (or grain coarsening)**: at high temperature above about $0.5 T_m$

Grain Growth (Soap Bubble Model)

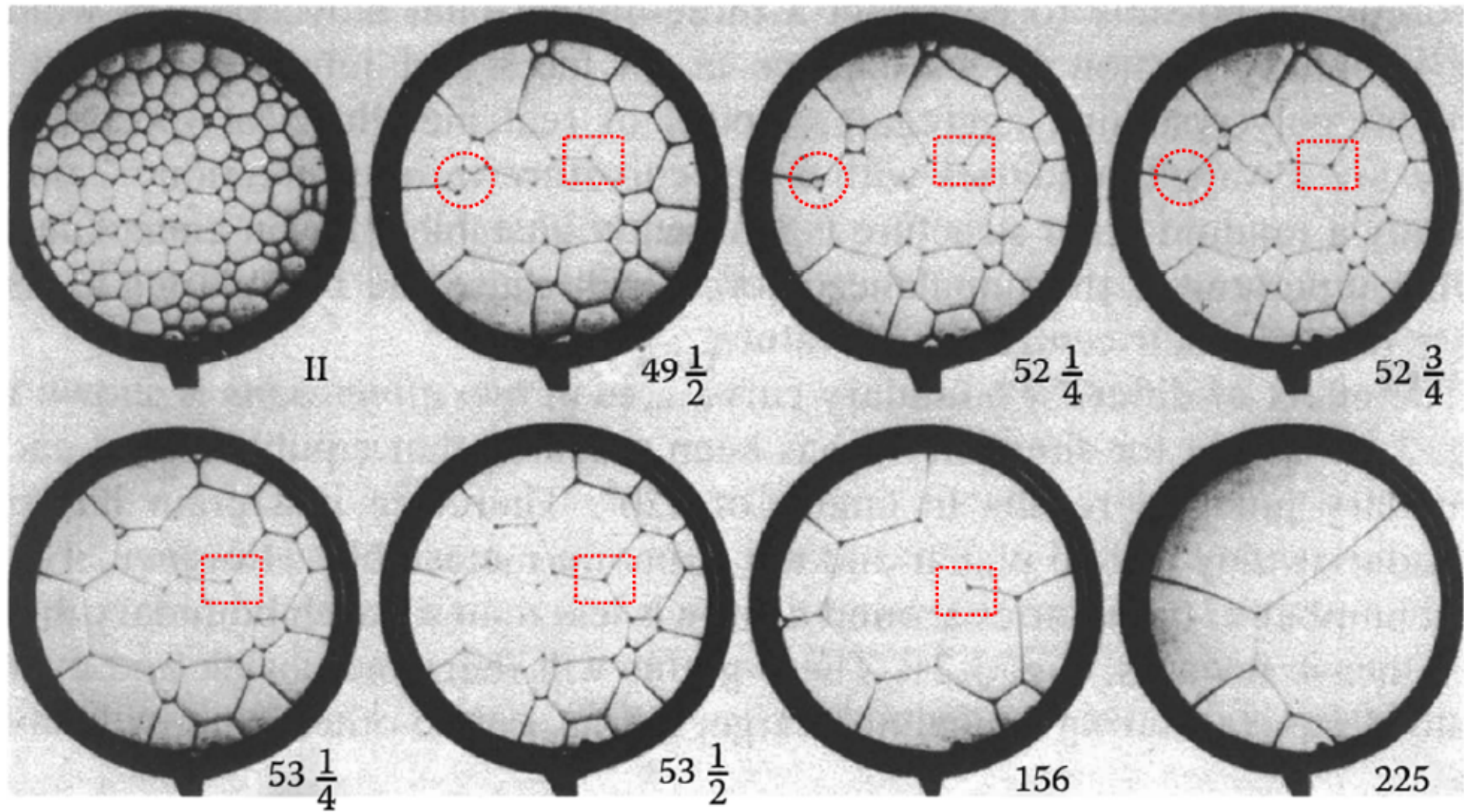
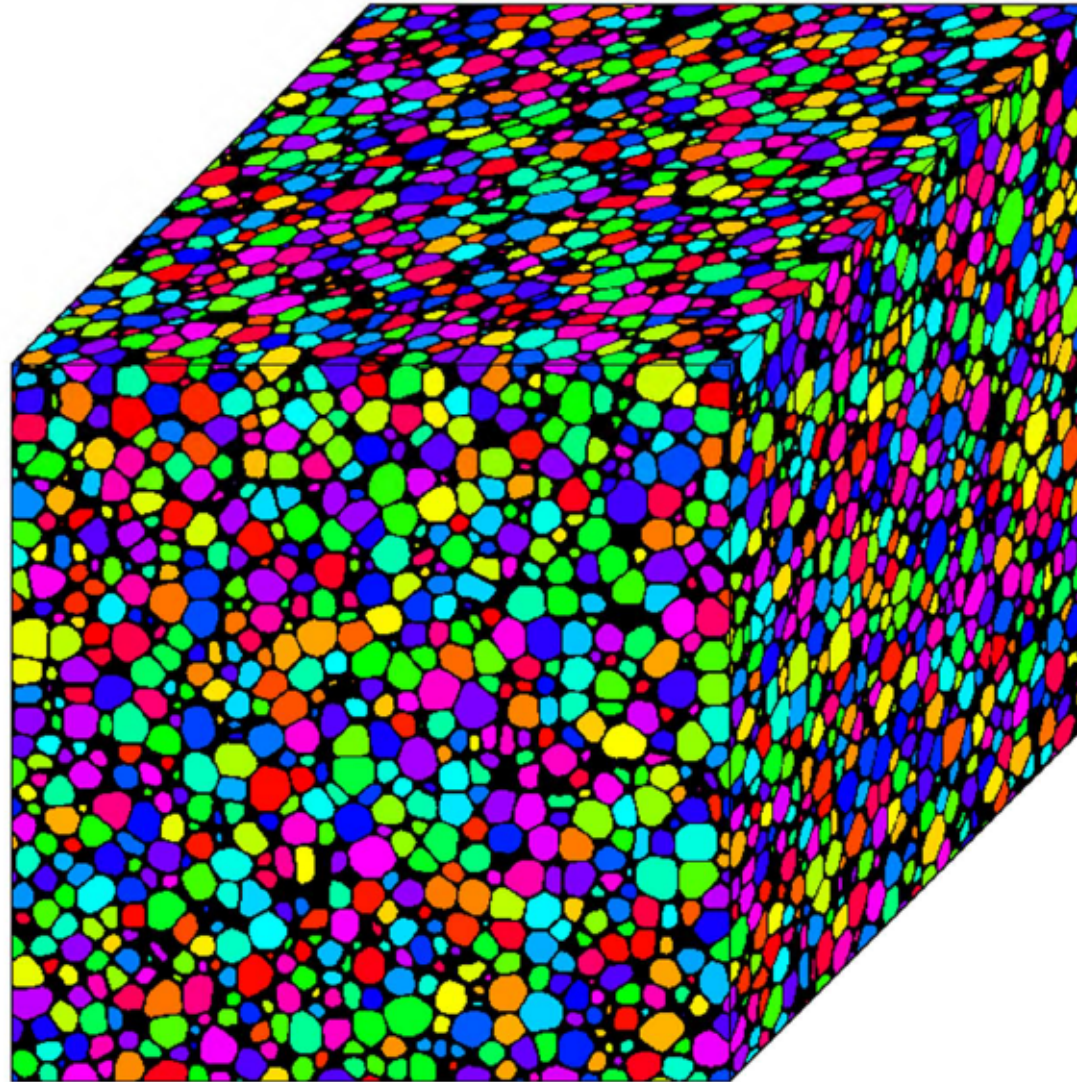


Fig. 3.22 Two-dimensional cells of a soap solution illustration the process of grain growth. Numbers are time in minutes.

Example of Grain Growth simulation in 3D



b) Grain Coarsening at High Temp. annealing (above about $0.5 T_m$):

The atoms in the shrinking grain detach themselves from the lattice on the high pressure side of the boundary and relocate themselves on a lattice site of the growing grain.

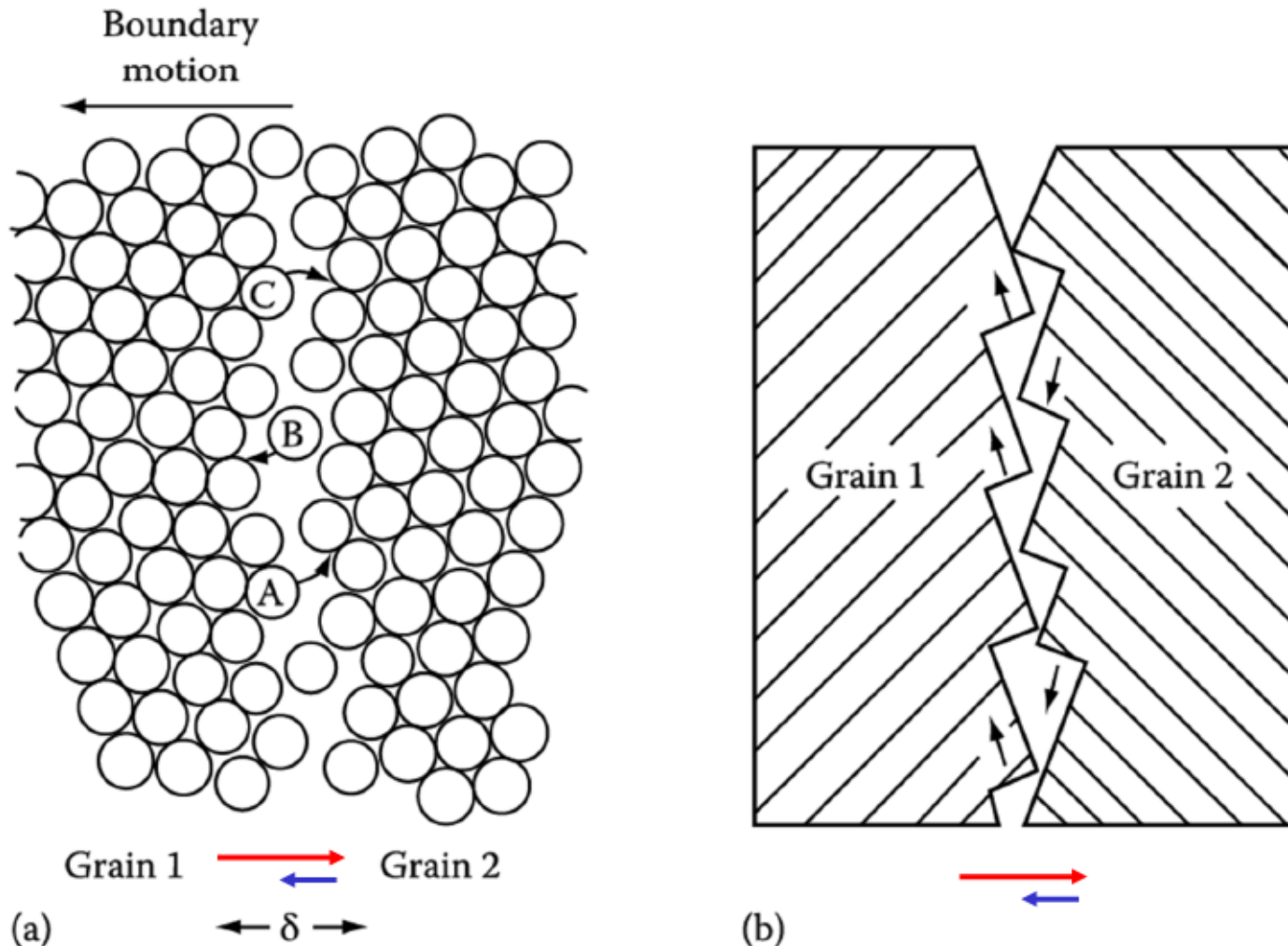


Fig. 3. 23 (a) The atomic mechanism of boundary migration. The boundary migrates to the left if the jump rate from grain 1 \rightarrow 2 is greater than 2 \rightarrow 1. Note that the free volume within the boundary has been exaggerated for clarity. (b) Step-like structure (돌출맥 구조) where close-packed planes protrude into the boundary.

* Grain coarsening at high T annealing curvature $\sim \Delta P \sim \Delta\mu$

→ metastable equilibrium state

: # ↓ , size ↑

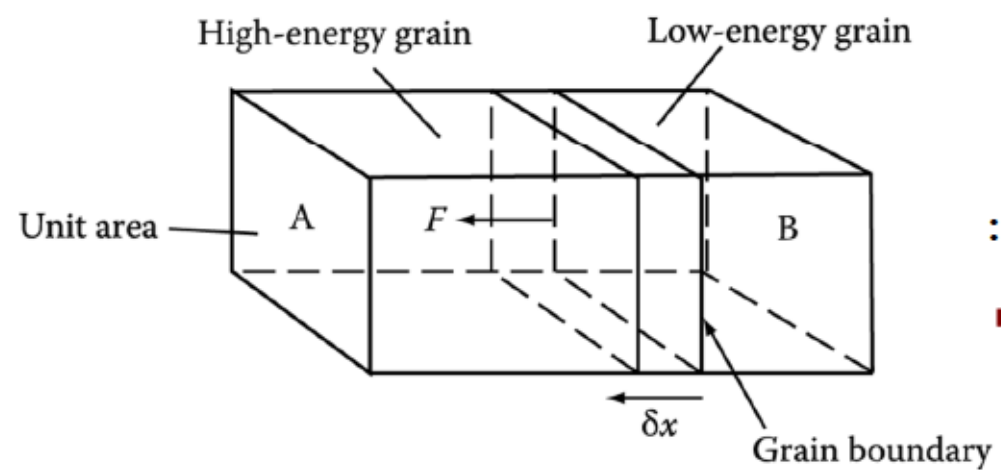
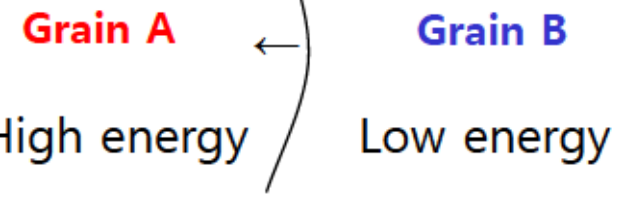


Fig. 3.25 A boundary separating grains with different free energies is subjected to a pulling force F.



$\Delta G = 2\gamma V_m / r \sim \Delta\mu$ Gibbs-Thomson Eq.
 : effect of pressure difference by curved boundary

➔ Driving force for grain growth : F

If unit area of GB advances a distance δx , # of moles of material that enter grain B

$$\delta x \cdot (1/V_m)$$

Work : $F dx = (2\gamma V_m / r) (\delta x / V_m)$

→ $F = 2\gamma / r = \Delta G / V_m$ (by curvature)

1) Pulling force per unit area of boundary : $F = \frac{\Delta G}{V_m}$ ($N m^{-2}$) (Eq. 3.18)

Applies equally to any boundary whose migration causes a decrease in free energy, i.e. during recrystallization, the boundaries btw the new strain-free grains and the original deformed grains

Free energy difference per unit volume

Q: Grain boundary (α/α interfaces)

(a) Low-Angle and High-Angle Boundaries

(b) Special High-Angle Grain Boundaries

(c) Equilibrium in Polycrystalline Materials

3) Kinetics of grain growth

- Grain boundary migration (v) by thermally activated atomic jump

Boundary velocity $v = \frac{A_2 n_1 v_1 V_m^2}{N_a RT} \exp\left(-\frac{\Delta G^a}{RT}\right) \frac{\Delta G}{V_m}$ $v \sim \Delta G/V_m$ driving force
 $\rightarrow F = \Delta G/V_m$

M : mobility = velocity under unit driving force $\sim \exp(-1/T)$

rate of grain growth $dD/dt \sim 1/D$, exponentially increase with T

$\rightarrow \underline{D} = k't^n$ (Experimental: $n \ll 1/2$, $1/2$ at pure metals or high Temp.)

- Mobility of GB \sim affected by both type of boundaries and GB segregation or 2nd phase precipitation

i.e Normal grain growth \longleftrightarrow Abnormal grain growth

2) How fast boundary moves? : Grain Growth Kinetics

Effect of the driving force on the kinetics of boundary migration

Grain boundary migration by thermally activated atomic jump

* (1) \rightarrow (2) : Flux

(1) atoms in probable site : n_1

Vibration frequency : ν_1

A_2 : probability of being accommodated in grain (2)

$$\rightarrow A_2 n_1 \nu_1 \exp(-\Delta G^a/RT) \text{ atom/m}^2\text{s} = J_{1\rightarrow 2}$$

* (2) \rightarrow (1) : Flux

$$\rightarrow A_1 n_2 \nu_2 \exp[-(\Delta G^a + \Delta G) /RT] = J_{2\rightarrow 1}$$

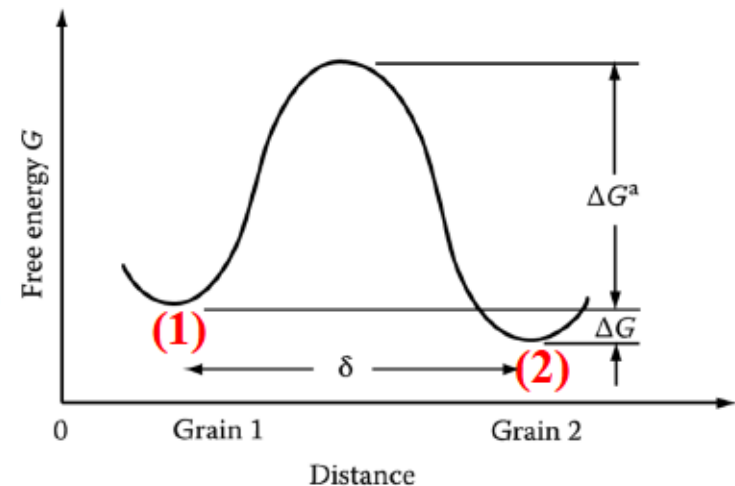
When $\Delta G=0$, there is **no net boundary movement**.

$$A_2 n_1 \nu_1 \approx A_1 n_2 \nu_2 = Anv$$

When $\Delta G > 0$, there will be a **net flux** from grain 1 to 2. (For a high-angle GB, $A_1 \approx A_2 \approx 1$)

$$(A_2 n_1 \nu_1 \approx A_1 n_2 \nu_2 = Anv)$$

$$J_{\text{net}} = J_{1\rightarrow 2} - J_{2\rightarrow 1} = Anv \exp(-\Delta G^a/RT) [1 - \exp(-\Delta G/RT)] \quad 51$$



$$J_{1 \rightarrow 2} - J_{2 \rightarrow 1} = A n v \exp(-\Delta G^a/RT) [1 - \exp(-\Delta G/RT)]$$

- If the boundary is moving with a velocity v , the above flux must also be equal to 순표류속도

$$J = v \cdot c_B \rightarrow v / (V_m / N_a) \quad (V_m / N_a : \text{atomic volume})$$

Diffusion flux

If ΔG is small [$\Delta G \ll RT$] \rightarrow Apply Taylor expansion to $\exp(-\Delta G/RT)$ term

$$J_{\text{net}} = A_2 n_1 v_1 \exp(-\Delta G^a/RT) [\Delta G/RT] \text{ (atom/m}^2\text{s)} = v / (V_m / N_a)$$

Boundary velocity $v = \frac{A_2 n_1 v_1 V_m^2}{N_a R T} \exp\left(-\frac{\Delta G^a}{RT}\right) \frac{\Delta G}{V_m}$ $v \sim \Delta G / V_m$ driving force

$\rightarrow F = \Delta G / V_m$

or $v = M \cdot \Delta G / V_m$ M : mobility of boundary, i.e., the velocity under unit driving force

$$\text{where } M = \left\{ \frac{A_2 n_1 v_1 V_m^2}{N_a R T} \exp\left(\frac{\Delta S^a}{R}\right) \right\} \exp\left(\frac{-\Delta H^a}{RT}\right)$$

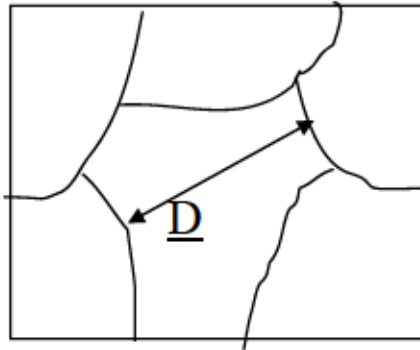
M : mobility = velocity under unit driving force $\sim \exp(-1/T)$
exponentially increase with temp

\Rightarrow The boundary migration is a thermally activated process.
(입계 이동은 확산처럼 열활성화 과정)

* Kinetic of grain growth

1) driving force $F = \Delta G/V_m$ → $v = M (\Delta G/V_m)$ **Boundary velocity**
Pulling force M : exponentially increase with temp.

v : relation to grain coarsening



Mean grain size (diameter) : \underline{D}

Mean radius of curvature of boundary : r

if $\underline{D} \propto r$,

$$\begin{aligned} \text{Mean velocity : } \underline{v} &= \alpha M (\Delta G/V_m) = d\underline{D}/dt \quad (\Delta G = 2\gamma V_m/r) \\ &= \alpha M(2\gamma/\underline{D}) = d\underline{D}/dt \quad (\alpha = \text{proportional constant} \sim 1) \end{aligned}$$

\underline{v} (rate of grain growth) $\sim 1/\underline{D}$, exponentially increase with T

Mean velocity : $\underline{v} = \alpha M (\Delta G/V_m) = d\underline{D}/dt$ ($\Delta G = 2\gamma V_m/r$)
 $= \alpha M (2\gamma/\underline{D}) = d\underline{D}/dt$ ($\alpha = \text{proportional constant} \sim 1$)

Integration of previous eq. from D_0 to \underline{D} ,

$$\rightarrow \int_{D_0}^{\underline{D}} \frac{d\underline{D}}{\underline{D}} = \int 2\alpha M \gamma dt$$

$$\rightarrow \frac{1}{2} (\underline{D}^2 - D_0^2) = 2\alpha M \gamma t$$

$$\rightarrow (\underline{D}^2 - D_0^2) = 4\alpha M \gamma t = kt$$

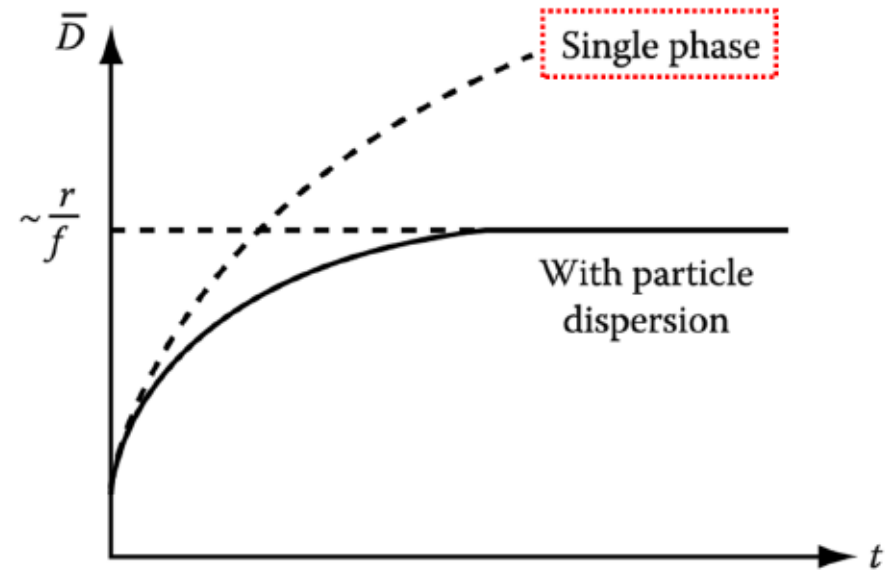
$$\rightarrow \underline{D}^2 = D_0^2 + kt$$

if $D_0 \approx 0 \rightarrow \underline{D} = k't^{1/2}$

$\rightarrow \underline{D} = k't^n$ (experimental : $n \ll 1/2$, $1/2$ in very pure metals or only high temp.)

Single phase

- \therefore the velocity of GB migration, v is not linear function of ΔG .
- $\rightarrow M$ is not a const. but varies with ΔG and thus also with D .
- \rightarrow Variation of M in alloys could arise from solute drag effects. (M in alloy is relatively slower than that of pure metal)



$r = \text{average radius of particles}$

$f_v = \text{volume fraction of particles}$

Whose mobility would be high between special and random boundaries?

By considering grain boundary structure,

(Mobility depending on GB structures)

High energy G.B. → relatively open G.B. structure → High mobility

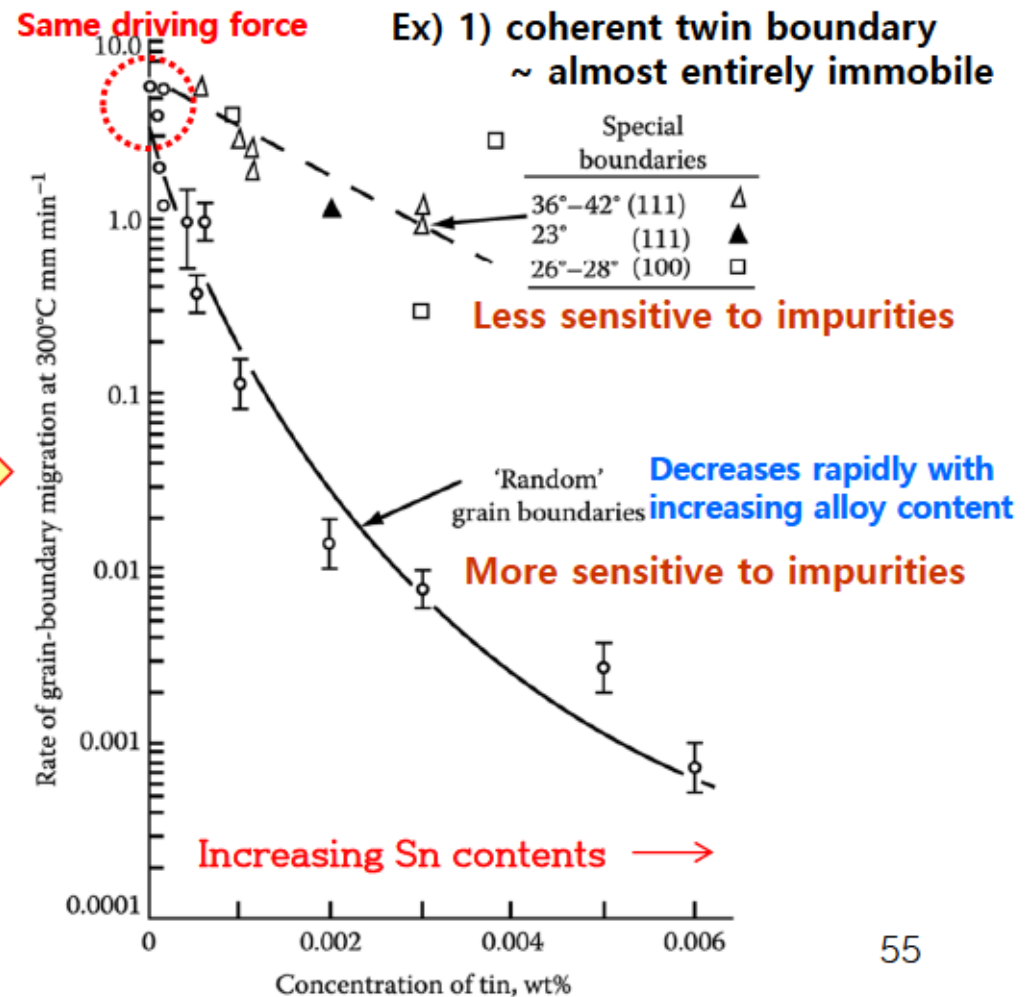
Low energy G.B. → closed (or denser) G.B. structure → Low mobility

But, **Ideal** ↔ **Real**

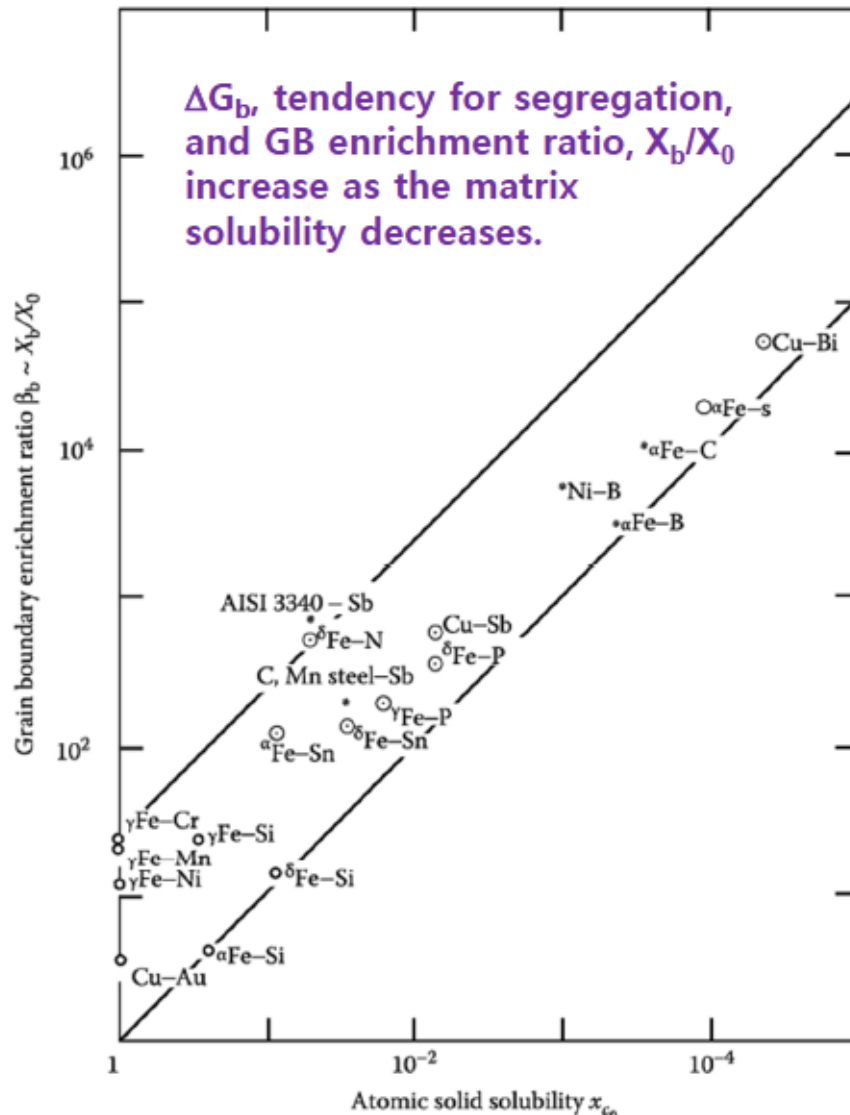
2) The other special boundaries are usually more mobile than random high-angle boundary. Why?

If the metal were "perfectly" pure the random boundaries would have the higher mobility.

⇒ Due to differences in the interactions of alloy elements or impurities with different boundaries



Migration rate of special and random boundaries at 300 °C in zone-refined lead alloyed with tin under equal driving forces



<Increasing GB enrichment with decreasing solid solubility in a range of system>

X_0 : matrix solute concentration/ X_b : boundary solute concentration

ΔG_b : free energy reduced when one mole of solute is moved to GB from matrix.

(ΔG_b) → The high mobility of special boundaries can possibly be attributed to a low solute drag on account of the relatively more close-packed structure of the special boundaries.

* Solute drag effect

In general, G_b (grain boundary E) and mobility of pure metal decreases on alloying.

~Impurities tend to stay at the GB.

Generally, ΔG_b , tendency of segregation, increases as the matrix solubility decreases.

$$X_b = X_0 \exp \frac{\Delta G_b}{RT}$$

X_b/X_0 : GB enrichment ratio

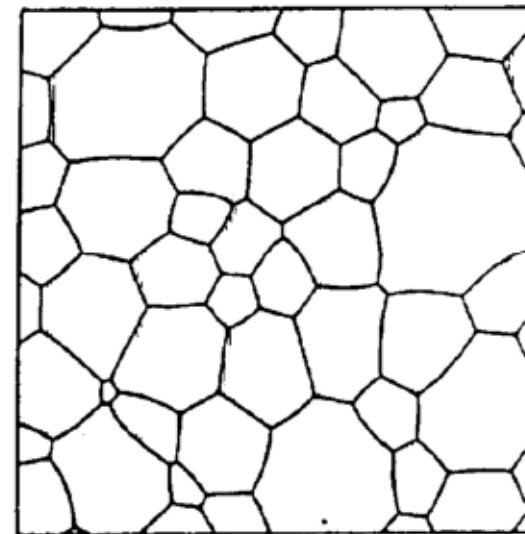
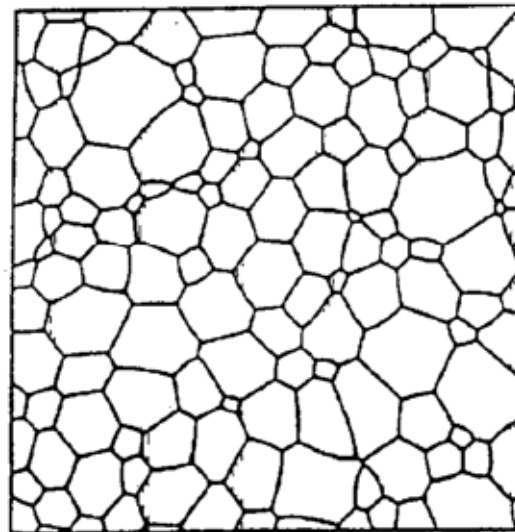
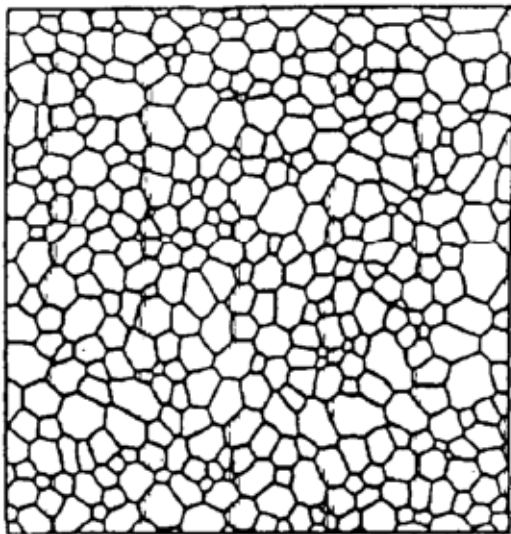
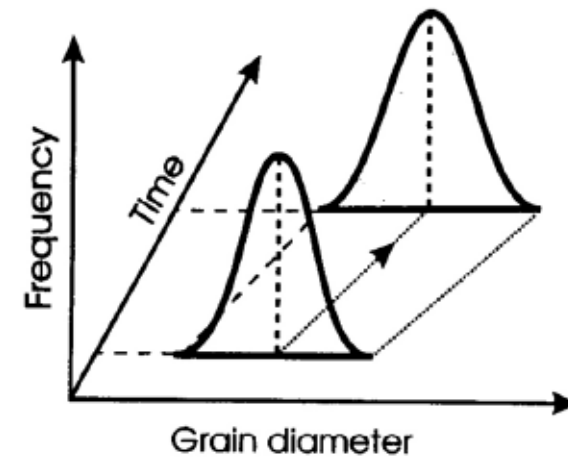
- Decreases as temp. increases, i.e., the solute "evaporates" into the matrix

Low T or ΔG_b ↑ X_b ↑ Mobility of G.B. ↓

→ Alloying elements affects mobility of G.B.

Normal Grain Growth

- Grain boundary moves to reduce area and total energy
- Large grain grow, small grains shrink
- Average grain size increases
- Little change of size distribution

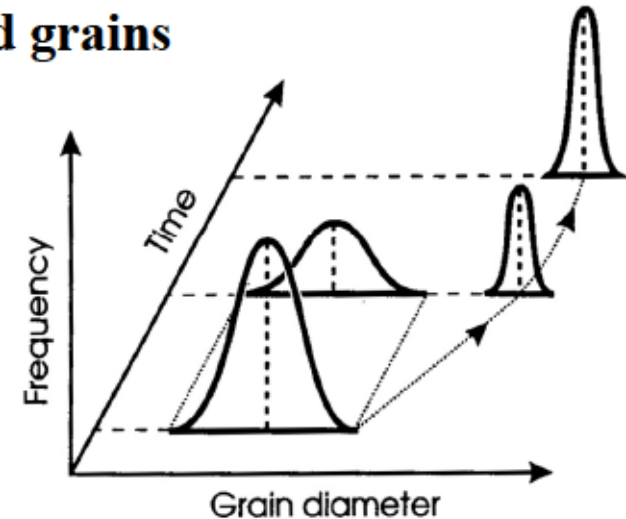


Abnormal Grain Growth

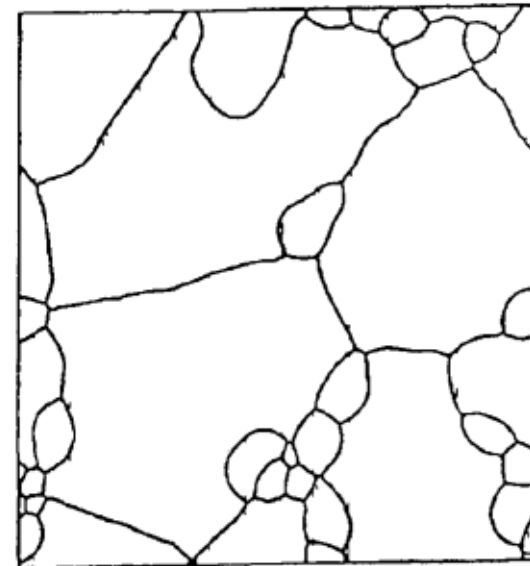
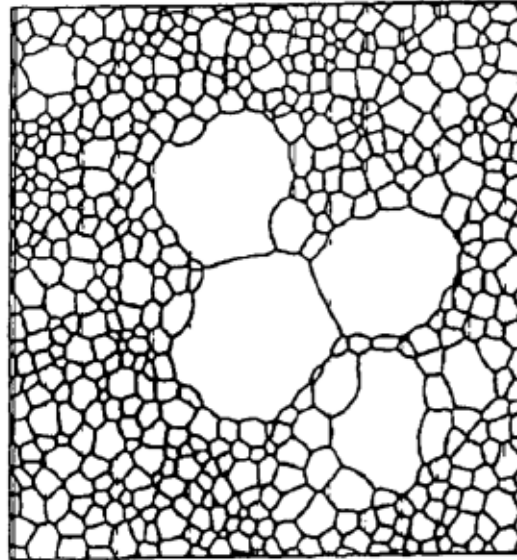
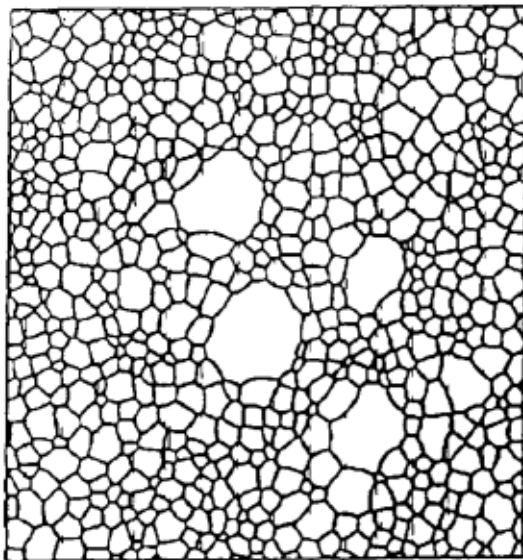
(high mobility of special GBs → development of recrystallization textures)

❑ Discontinuous grain growth of a few selected grains

- Local breaking of pinning by precipitates
- Anisotropy of grain boundary mobility
- Anisotropy of surface & grain boundary energy
- Selective segregation of impurity atoms
- Inhomogeneity of strain energy



❑ Bimodal Size distribution



Abnormal Grain Growth

ex) Si steel → improvement of “soft magnetic property”
= discontinuous grain growth or secondary recrystallization

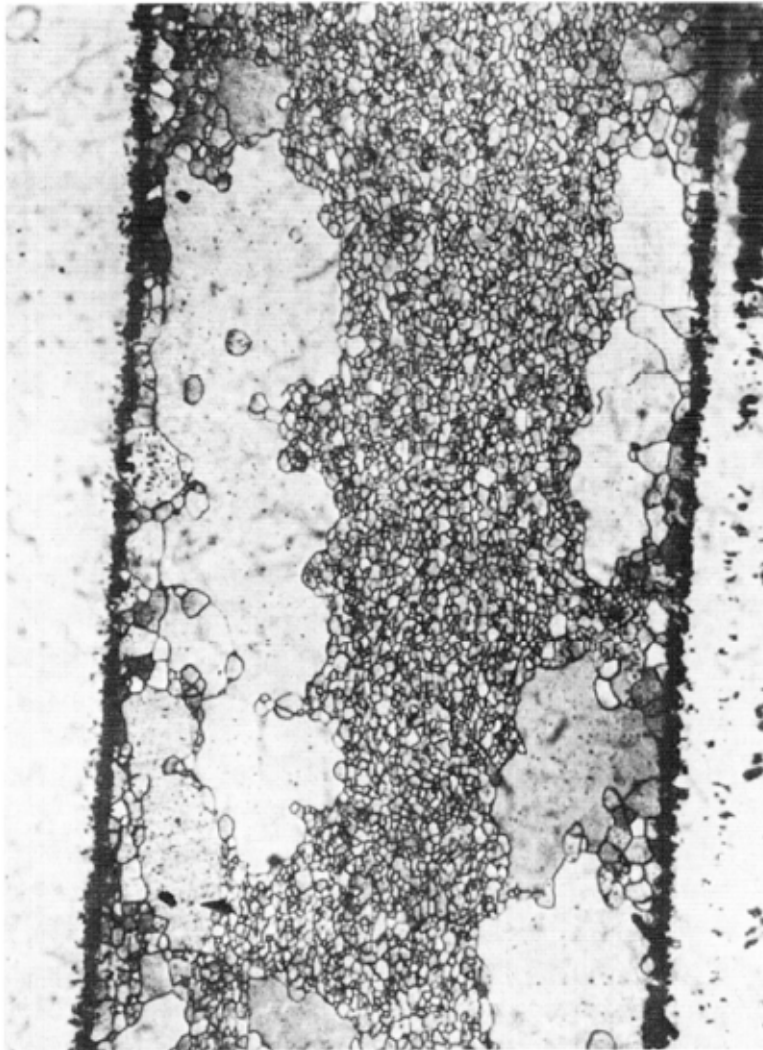


Figure 5.87 Optical micrograph showing abnormal grain growth in a fine grain steel containing 0.4 wt% carbon. The matrix grains are prevented from growing by a fine dispersion of carbide particles that are not revealed. Magnification $\times 135$. (After Gawne and Higgins 1971. Courtesy of the Metals Society.)

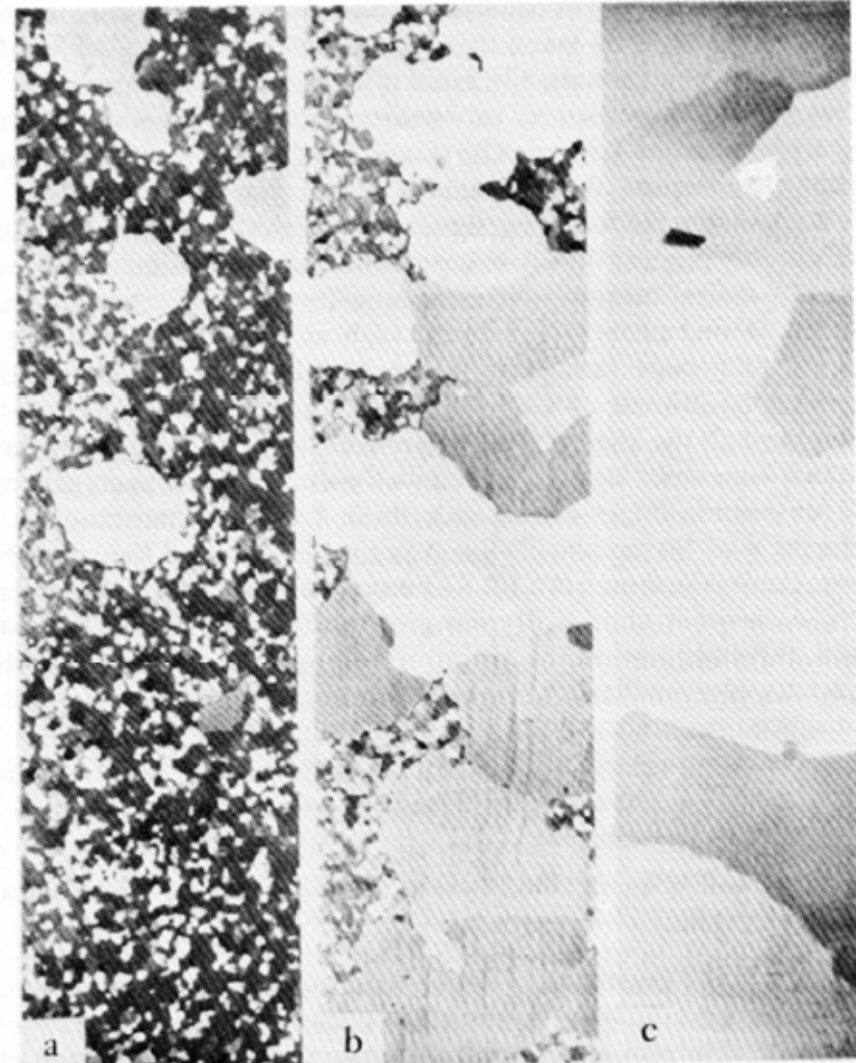


Fig. 5.48. Evidence for the preferential formation of (110)[001]-oriented grains by secondary recrystallization in 5% Si-Fe (Graham [1969]).

Q: Grain boundary (α/α interfaces) = Boundaries in Single-Phase Solids

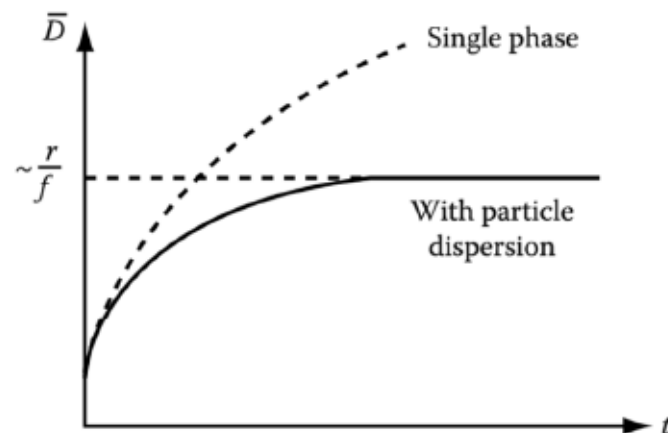
(a) Low-Angle and High-Angle Boundaries

(b) Special High-Angle Grain Boundaries

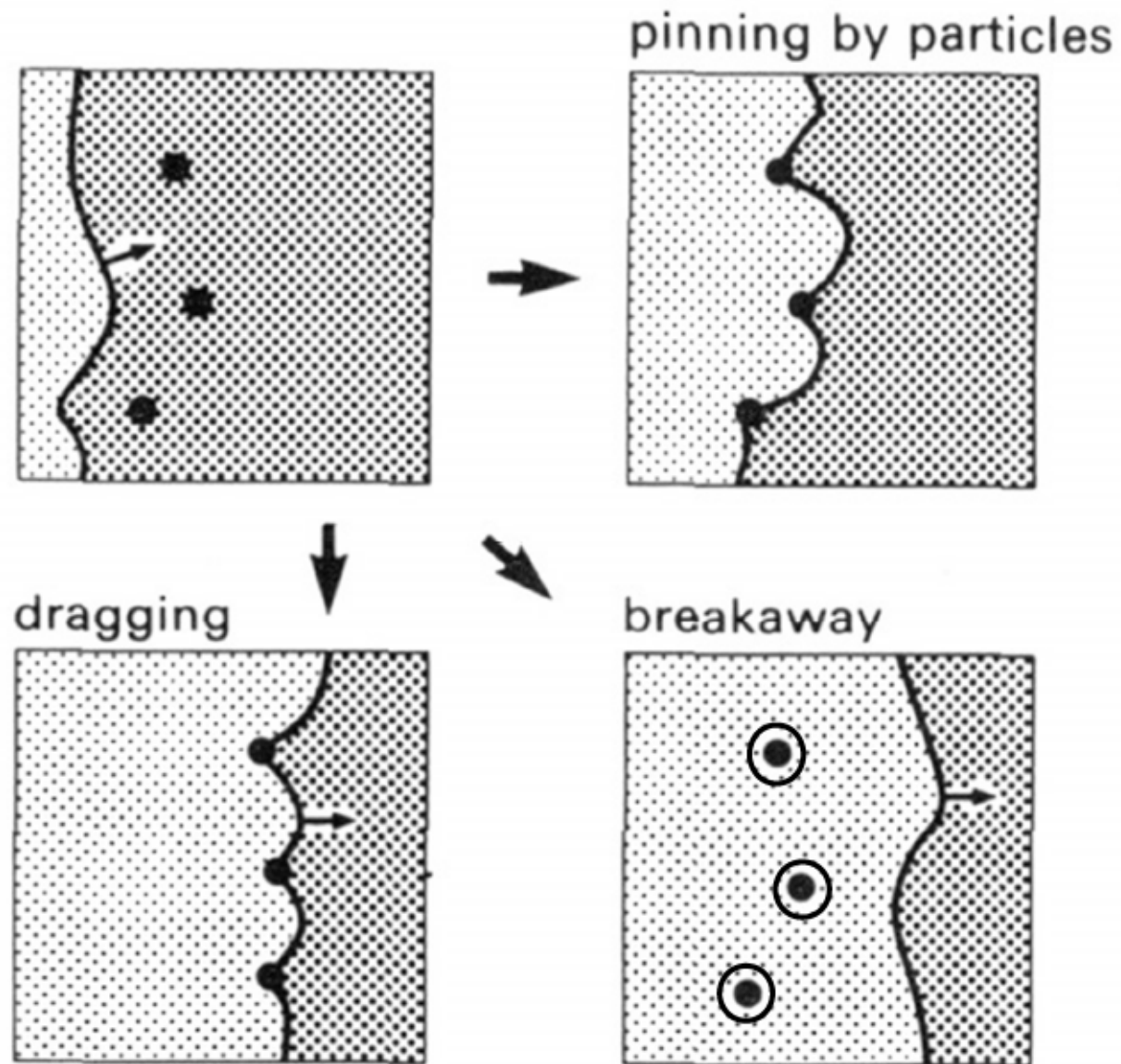
(c) Equilibrium in Polycrystalline Materials

4) Effect of second-phase particle on GB migration : Zener Pinning

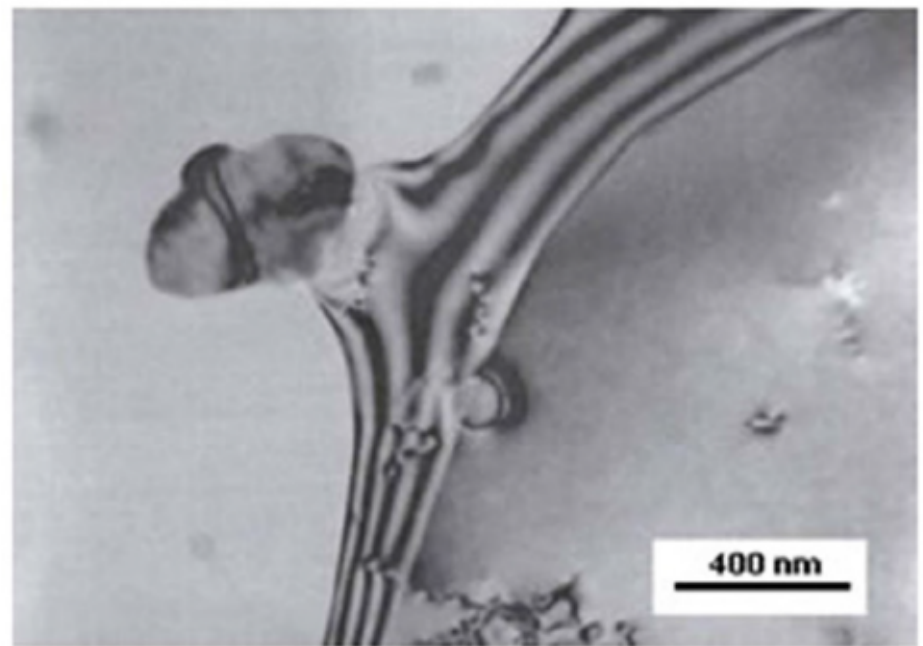
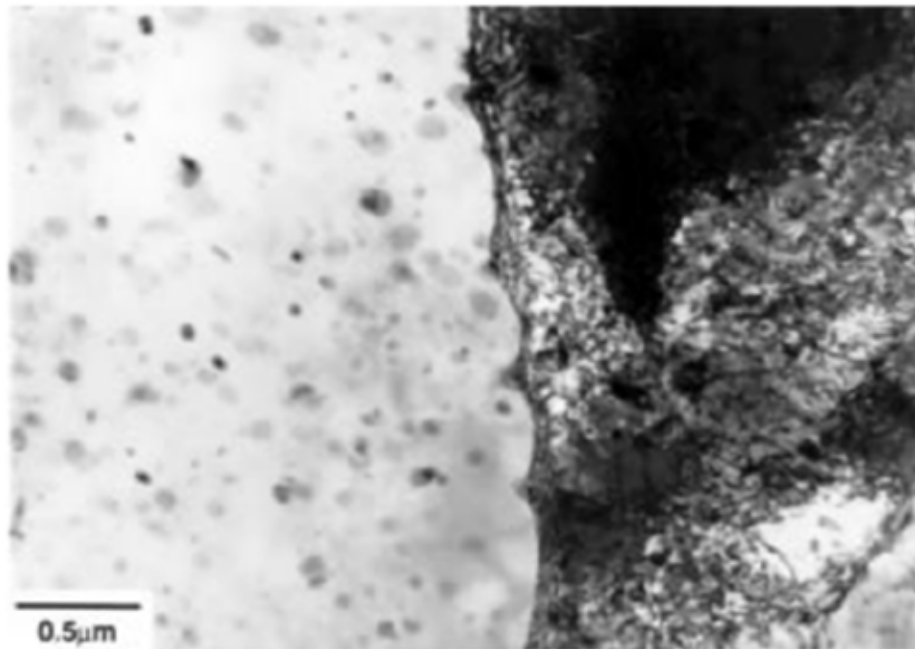
$$\bar{D}_{\max} = \frac{4r}{3f_v}$$



Schematic diagram illustrating the possible interactions of second phase particles and migrating grain boundaries.



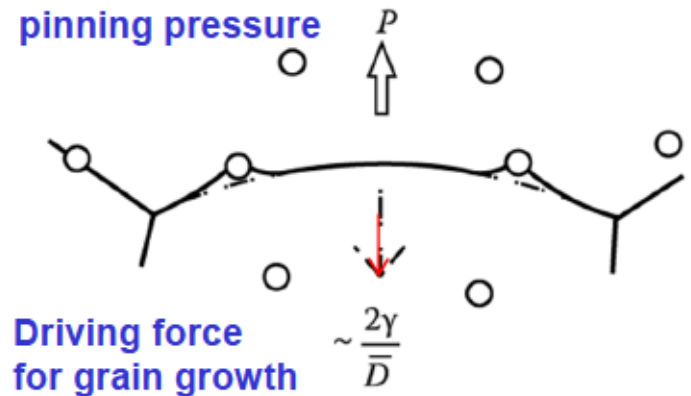
Pinning by particle



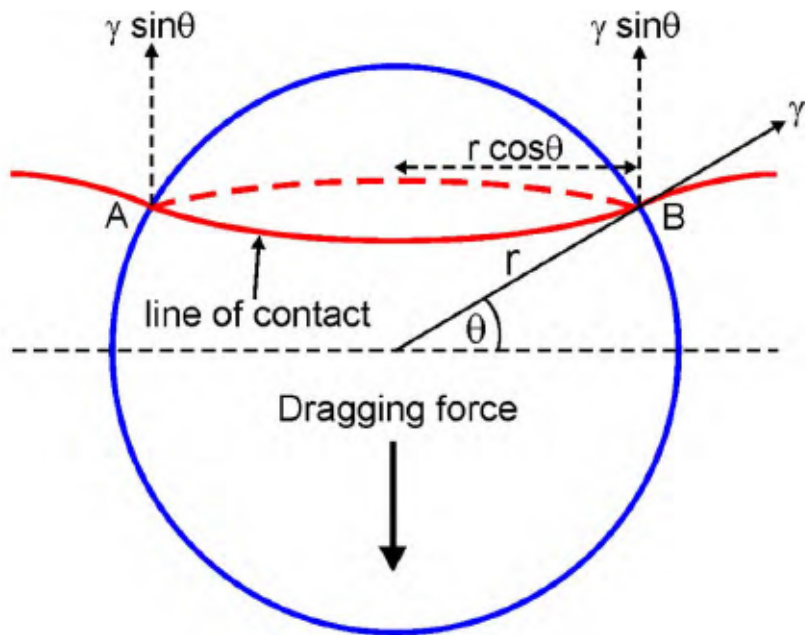
제 2 상이 존재할 때 결정립의 성장

Effect of Second-Phase Particles on GB migration

Interaction with particles **Zener Pinning**



Derive the expression for the pinning effect of grain boundary migration by precipitates.



since $\gamma \sin\{\theta\} = \text{force per unit length}$

$$F = \gamma \sin\{\theta\} \times \underbrace{2\pi r \cos\{\theta\}}_{\text{circumference}} = AB$$

so that at $\theta = 45^\circ$

$$F_{max} = \gamma\pi r$$

Maximum force exerted by a single particle

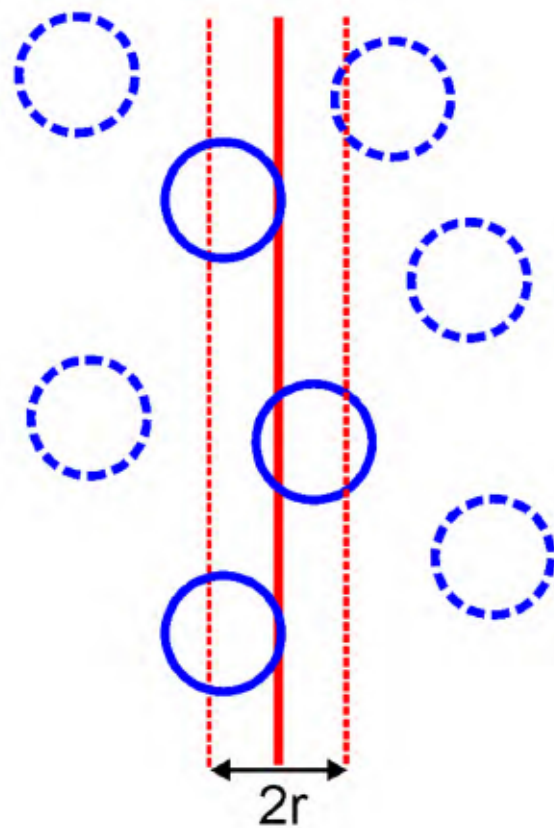
Interaction with particles

Zener Pinning

f_v = volume fraction of randomly distributed particles of radius r

N_{total} = number of particles per unit volume

$$N = \frac{f_v}{\frac{4}{3}\pi r^3}$$



Only particles within one radius (solid circles) can intersect a planar boundary

If the boundary is essentially planar,

$$N_{\text{interact}} = 2rN_{\text{total}} = 3f_v/2\pi r^2$$

Mean # of particles intersecting unit area of a random plane

Given the assumption that

all particles apply the maximum pinning force,

the total pinning pressure

$$P = \frac{3f_v}{2\pi r^2} \cdot \pi r \gamma = \frac{3f_v \gamma}{2r}$$

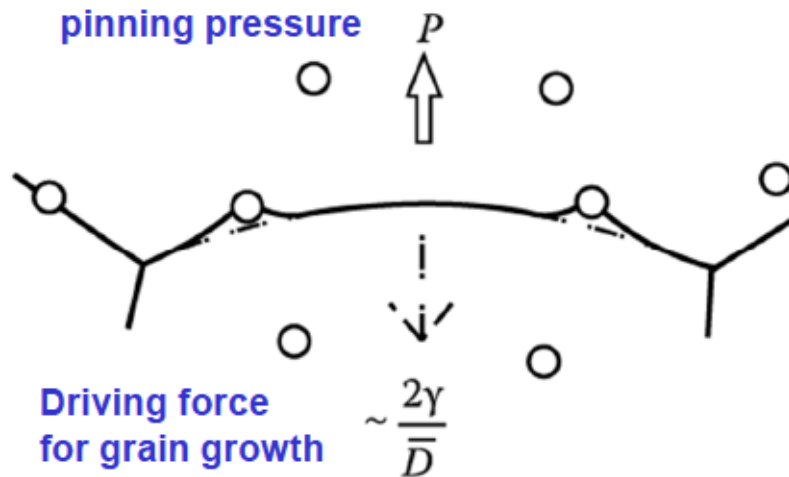
This force will oppose the driving force for grain growth, $\frac{2\gamma}{\bar{D}}$.

Interaction with particles

Zener Pinning

$$P = \frac{3f_v}{2\pi r^2} \cdot \pi r \gamma = \frac{3f_v \gamma}{2r}$$

This force will oppose the driving force for grain growth, $2\gamma/\bar{D}$.



$$\rightarrow F = 2\gamma/r = \Delta G/V_m \text{ (by curvature)}$$

$$\frac{2\gamma}{\bar{D}} = \frac{3f_v \gamma}{2r} \rightarrow \bar{D}_{\max} = \frac{4r}{3f_v}$$

Driving force will be insufficient to overcome the drag of the particles and grain growth stagnates.

For fine grain size

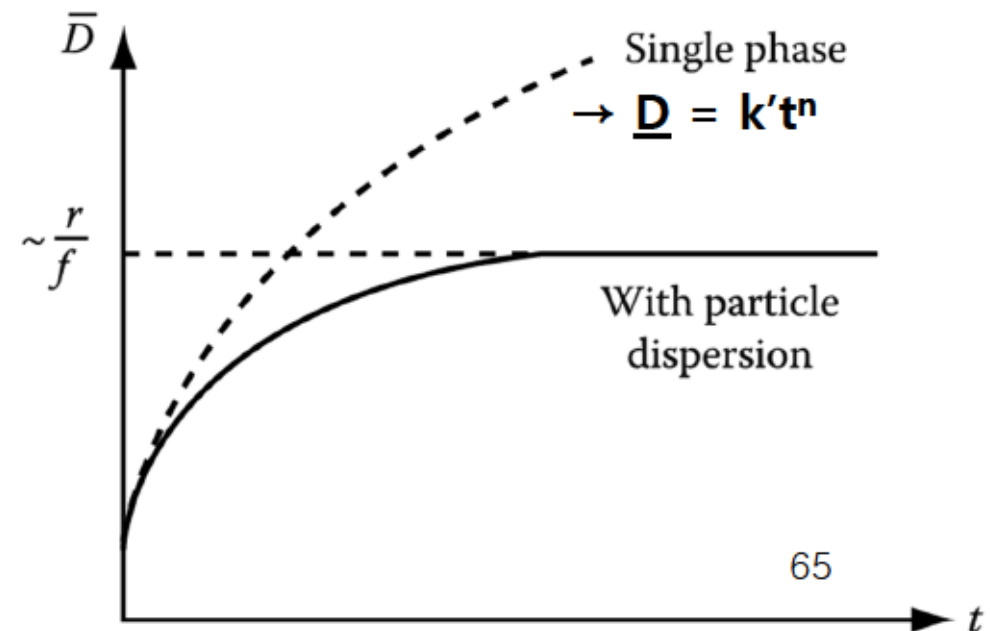
\rightarrow a large volume fraction of very small particles

* Effect of second-phase particles on grain growth

$$\bar{D}_{\max} = \frac{4r}{3f_v}$$

: Stabilization of a fine grain size during heating at high temp. \rightarrow large volume fraction ($f \uparrow$) of very small particles ($r \downarrow$).

$$\bar{D}_{\max} = \frac{4r}{3f_v} \downarrow$$



Summary for today's class

- **Thermally Activated Migration of Grain Boundaries:**

Metastable equilibrium of grain boundary (Balances of 1) boundary E + 2) surface tension)

→ real curvature ($\Delta P \rightarrow \Delta G$: Gibbs Thomson Eq.) → $F = 2\gamma/r = \Delta G/V_m$ (by curvature)

(Pulling force per unit area of boundary)

→ Grain coarsening at high T annealing

- **Kinetics of Grain Growth**

- Grain boundary migration (v) by thermally activated atomic jump

Boundary velocity $v = \frac{A_2 n_1 v_1 V_m^2}{N_a RT} \exp\left(-\frac{\Delta G^a}{RT}\right) \frac{\Delta G}{V_m}$

$v \sim \Delta G/V_m$ driving force
→ $F = \Delta G/V_m$

M : mobility = velocity under unit driving force $\sim \exp(-1/T)$

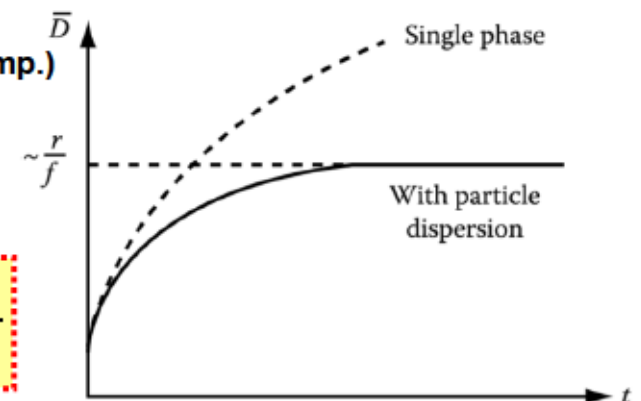
rate of grain growth $d\bar{D}/dt \sim 1/\bar{D}$, exponentially increase with T

→ $\bar{D} = k't^n$ (Experimental: $n \ll 1/2$, $1/2$ at pure metals or high Temp.)

- Mobility of GB \sim affected by both type of boundaries and GB segregation or 2nd phase precipitation

Ex) Effect of second-phase particle - Zener Pinning

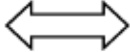
$$\bar{D}_{\max} = \frac{4r}{3f_v}$$



Summary for today's class

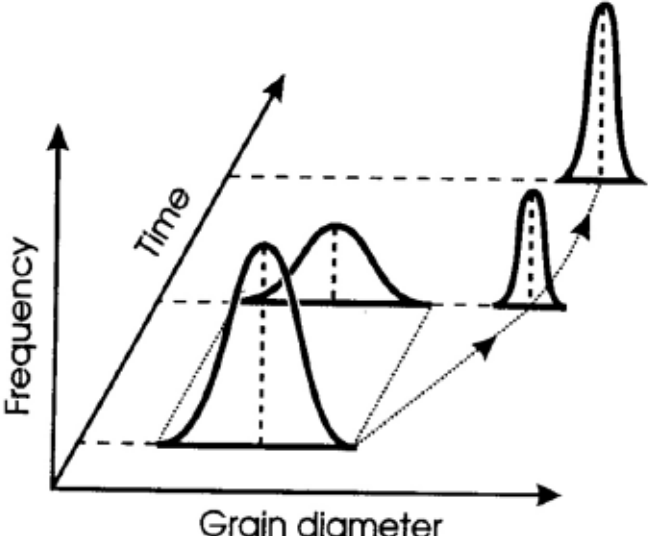
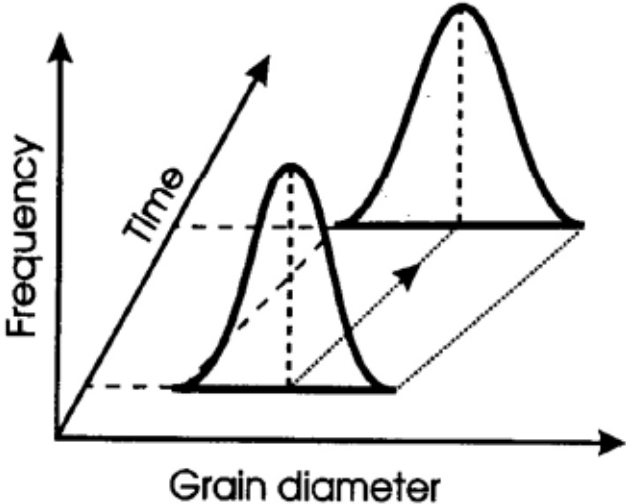
- Grain Growth**

- Normal grain growth

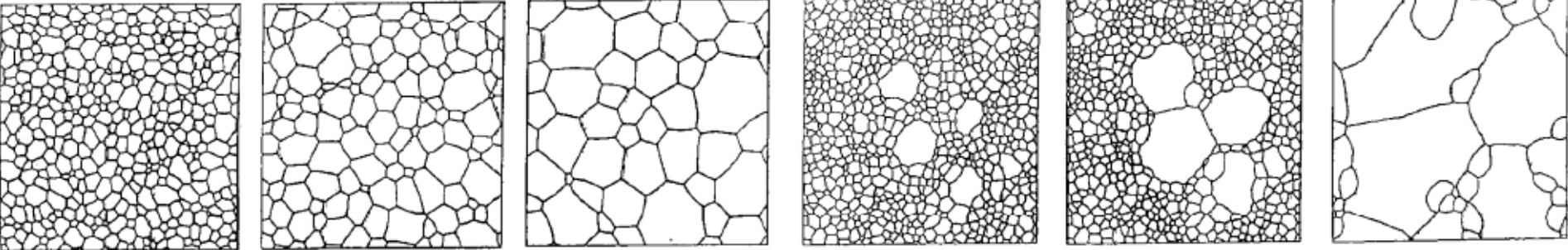


Abnormal grain growth

(high mobility of special GBs
→ development of recrystallization textures)



< Bimodal Size distribution >



MIDTERM (3rd November, 4 PM-7 PM)

Scopes: Text ~ page 146 (~ chapter 3.3)/

Teaching notes: 1~11/

and Homeworks

Places: 33-327 (class #: 1-25) & 330 (class #: 26-50)

Good Luck!!